JGR Oceans

RESEARCH ARTICLE
10.1029/2022JC018870

The Freshwater Balance of the Adriatic Sea: A Sensitivity Study

Martin Vodopivec[1], Klodian Zaimi[2], and Álvaro J. Peliz[3]

[1]Marine Biology Station Piran, National Institute of Biology, Piran, Slovenia, [2]Department of Hydrology, Institute of GeoSciences, Polytechnic University of Tirana, Tirana, Albania, [3]Instituto Dom Luis, Faculdade de Ciências da Universidade de Lisboa, Lisboa, Portugal

Key Points:

- The positive-feedback mechanism amplifies the Adriatic sensitivity to freshwater balance
- The freshwater budget depends on poorly constrained river runoff as well as on the choice of atmospheric forcing
- Different model configurations lead to considerable differences in circulation and water exchange between the Adriatic and Ionian Sea

Correspondence to:
M. Vodopivec,
martin.vodopivec@nib.si

Citation:
Vodopivec, M., Zaimi, K., & Peliz, Á. J. (2022). The freshwater balance of the Adriatic Sea: A sensitivity study. *Journal of Geophysical Research: Oceans*, *127*, e2022JC018870. https://doi.org/10.1029/2022JC018870

Received 20 MAY 2022
Accepted 28 OCT 2022

Abstract The Adriatic Sea is a narrow semi-enclosed basin with considerable freshwater inflow, connected to the saltier Mediterranean Sea through a narrow strait. The northern and central parts of the basin are characterized by a shallow shelf, while the southern part features a pit exceeding 1,200 m in depth. We conducted a series of modeling experiments over a 16-year period (2000–2015) using different runoff configurations and different sources of atmospheric forcing to investigate the sensitivity of the Adriatic Sea circulation and hydrology to freshwater balance and heat loss. Our results show that the shelf salinity and the salinity of the surface layers in the southern Adriatic are part of a self-amplifying loop involving dense water formation, water exchange with the Mediterranean Sea, and salty water intrusions to the shelf. Therefore, the characteristics of the basin and the water circulation are highly sensitive to the freshwater budget and heat losses. River discharge is subject to large interannual variations and is poorly known for many of the Adriatic freshwater sources. To improve the accuracy of the freshwater budget, we created a new climatology for three Albanian rivers and modulated the monthly climatological discharge in accordance with the rivers Po and Isonzo (Soča). Evaporation, precipitation, and heat losses vary strongly among the available atmospheric reanalyses and we show that the choice of atmospheric forcing has a substantial impact on the hydrology and circulation of the Adriatic Sea.

Plain Language Summary The Adriatic Sea is a well-known dense water (DW) formation site with the densest water forming in the northern part of the basin. Our modeling experiments show that the salinity of the surface water in the Adriatic Sea has a strong influence on DW formation and on circulation down to the bottom of the deepest part of the basin. The model proves to be very sensitive to freshwater input (rivers, precipitation) and evaporation, as well as to heat losses during strong wind events, which means that the implementation of river runoff and the choice of atmospheric forcing have a decisive influence on the water exchange between the Adriatic and the Mediterranean Sea and the behavior of the whole Adriatic basin down to the deepest layers. The differences between model runs are considerable and can reach an order of magnitude for some variables.

1. Introduction

The Adriatic Sea is a semi-enclosed elongated basin in the northern part of the eastern Mediterranean Sea (Figure 1). It measures roughly 800 km in length and is about 200 km wide. The Adriatic features significant freshwater inflow which accounts for 1/3 of the total Mediterranean inflow. The largest tributary is river Po, located in the northern part of the basin, while about 2/3 of the freshwater input is distributed between many rivers and groundwater submarine springs (Janeković et al., 2014; Raicich, 1994; Verri et al., 2018). The northern and central Adriatic are characterized by a shallow shelf (about 30 and 100 m deep, respectively), while in the southern Adriatic the bathymetry drops below 1,200 m. The basin is connected to the Mediterranean Sea through the Strait of Otranto (OT - Figure 1) which features a 700 m deep sill. The Adriatic is a well-known dense water (DW) formation site (Pinardi et al., 2006). The northern Adriatic is the northernmost part of the Mediterranean Sea and, due to its shallow depth and intensive cold spells, it produces the densest water in the Mediterranean Sea (Cushman-Roisin et al., 2001).

The water between the Adriatic and the Mediterranean Sea is exchanged through the Strait of Otranto. This exchange is part of a feedback mechanism called the Adriatic-Ionian Bimodal Oscillating System or BiOS (Gačić et al., 2010). The properties of the water flowing into the Adriatic basin depend on the circulation in the Ionian

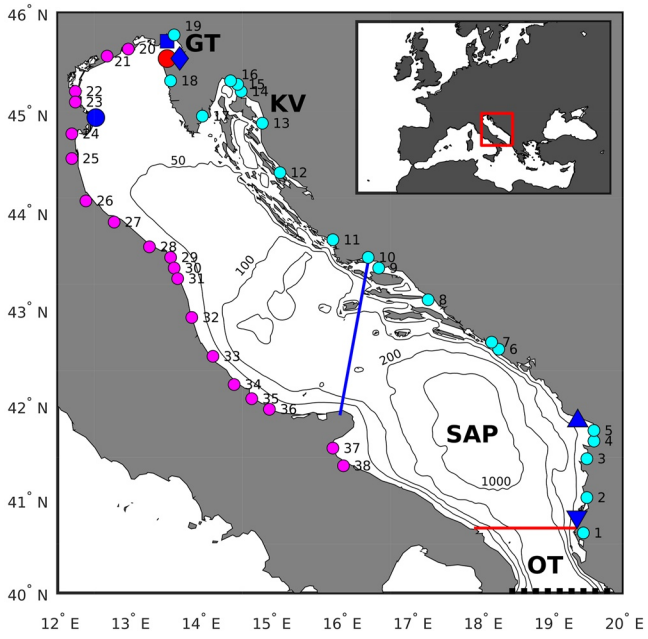

Figure 1. Map of the model domain (Adriatic Sea). Isobaths are plotted at 50, 100, 200, and 1,000 m depths. 'GT' marks the Gulf of Trieste, 'KV' Kvarner Bay, 'SAP' Southern Adriatic Pit, and 'OT' marks the Strait of Otranto. Red dot marks the location of Vida oceanographic buoy. The red and blue lines represent the Strait of Otranto and Palagruža sill transects respectively (118 and 214 km in length). The open boundary is located at the bottom edge of the image (40°N, below 'OT', marked with a dotted black line). The locations of the following river-mouths are marked in blue color: Po (circle), Isonzo (square), Rižana (diamond), Buna (upward triangle), Seman (downward triangle). The rest of the rivers with modulated climatological runoff are marked in magenta (modulated with Po) and cyan (modulated with Isonzo): 1 Vjose, 2 Shkumbin, 3 Erzen, 4 Ishem, 5 Mat, 6 HPP Kupari, 7 Ombla, 8 Neretva, 9 Cetina, 10 Jadro, 11 Krka, 12 Zrmanja, 13 HPP Senj, 14 Crikvenica, 15 Bakarac, 16 Rječina, 17 Raša, 18 Mirna, 19 Timavo, 20 Tagliamento, 21 Piave, 22 Brenta, 23 Adige, 24 Po diVolano, 25 Reno, 26 Foglia, 27 Metauro, 28 Esino, 29 Musone, 30 Potenza, 31 Chienti, 32 Tronto, 33 Pescara, 34 Sangro, 35 Trigno, 36 Biferno, 37 Cervaro, 38 Ofanto.

Sea. When the circulation is cyclonic, the inflowing water is of Eastern Mediterranean origin and of high salinity; when the circulation in the Ionian Sea is anticyclonic, the inflowing water is coming from the Western Mediterranean (Modified Atlantic Water) and of lower salinity. On the other hand, when the DW flowing out of the Adriatic Sea is of low density it causes doming of the isopycnals in the Ionian and favors cyclonic circulation and vice versa. These processes form an oscillating mechanism that causes reversals of Ionian circulation on a decadal scale (Gačić et al., 2021).

The Adriatic Sea has a rich history of ocean modeling which began in the early 1970s and has been thoroughly reviewed by Cushman-Roisin et al. (2001). There have been several long term modeling studies focusing on general circulation (Dunić et al., 2018, 2019; Mantziafou & Lascaratos, 2008; Oddo & Guarnieri, 2011; Pranić et al., 2021), and most of them on the DW formation as well, while some other studies focused solely on the latter (Bergamasco et al., 1999; Querin et al., 2013; Vested et al., 1998; Vilibić et al., 2016). Often the models were employed to study specific processes, such as tides (Cushman-Roisin & Naimie, 2002; Malačič et al., 2000), storm surges (Bressan et al., 2017; Ferrarin et al., 2020), circulation during strong wind events (Ličer et al., 2020; Malačič et al., 2012), meteotsunamis (Denamiel, Tojčić, & Vilibić, 2022), or effects of future climate change (Denamiel et al., 2020).

Currently, there are several operational models providing forecasts for the Adriatic, with horizontal resolution ranging from 1 to 4 km: 1 km NEMO model provided by the Slovenian Environment Agency (Ličer et al., 2020); 2 km AdriaROMS 4.0 system (Russo et al., 2013); 2.2 km AREG based on Princeton Ocean Model (Oddo et al., 2005); 2 km ROMS (Janeković et al., 2014) running at the Croatian Meteorological and Hydrological Service; Tiresias system based on the unstructured grid SHYFEM model with varying horizontal resolution from 7 km to tens of meters (Ferrarin et al., 2019); 4 km Mediterranean Forecasting System (MFS) providing the forecast for the whole Mediterranean Sea (Pinardi et al., 2003).

An extremely strong and long-lasting cold air outbreak (CAO) event in February 2012 produced the densest water ever observed in the Adriatic Sea (Mihanović et al., 2013) and inspired a series of modeling studies (Benetazzo et al., 2014; Carniel, Benetazzo, et al., 2016; Carniel, Bonaldo, et al., 2016; Janeković et al., 2014; Ličer et al., 2016; Mihanović et al., 2019; Querin et al., 2016; Ricchi et al., 2016; Vilibić et al., 2016). This extremely dense water with potential density anomaly (PDA) above 30 kg/m^3 (Mihanović et al., 2013) formed in the area spanning from the Gulf of Trieste to the Po river delta (Figure 1). The models reveal that the newly formed DW traveled southwards, and a part of the DW current filled the bottom of the Southern Adriatic Pit (SAP), while the lower density DW exited the Adriatic basin and entered the Ionian Sea (Querin et al., 2013) through the Strait of Otranto (Figure 1).

Numerous rivers and underwater springs flow into the Adriatic basin and outflow measurements are available only for a few of them. River discharges are usually obtained from water level measurements by using the Rating Curve method. The rating curves have to be continuously recalibrated and the interpolations and extrapolations introduce errors in discharge estimations (Dottori et al., 2009). Furthermore, the data are often not publicly available. Therefore, most of the modeling studies used the Raicich river climatology (Raicich, 1994), which has been shown to overestimate the freshwater input in the eastern part of the basin (Janeković et al., 2014; Vilibić et al., 2016). We employed the new monthly climatology of the Adriatic rivers (Vilibić et al., 2016) and compiled our climatology of the Albanian rivers in our efforts to improve the accuracy of freshwater balance in the basin. The discharge of the Adriatic rivers displays high interannual variations (Cozzi & Giani, 2011), and Vilibić et al. (2016) found little difference in DW formation in central and northern Adriatic when using real versus climatological runoff. This might not be true at least for the exceptionally dry or wet periods and other

ocean processes. We used the available measurements and modulated the climatological freshwater input with measured runoff.

The highly complex orography of the Adriatic Sea, with its numerous islands and mountain ranges surrounding the basin, has a considerable effect on the weather in this area, especially on wind direction and speed (Cavaleri & Bertotti, 1997; Signell et al., 2005). Therefore, the horizontal resolution has usually been the primary criterion in choosing the right atmospheric forcing for the models of the Adriatic Sea. In the last years, several atmospheric long term reanalyses have been made publicly available with the horizontal resolution approaching the dimensions that could resolve many of the key features in the Adriatic orography (Bazile et al., 2017; Bollmeyer, 2015). We study the wind in these reanalyses and also the freshwater exchange between the atmosphere and the ocean and their influence on the Adriatic circulation.

We build upon the work of Verri et al. (2018) and Vilibić et al. (2016) who used numerical simulations to study the influence of runoff on dense water (DW) formation and overturning circulation. Our work takes into account the whole freshwater balance, including evaporation and precipitation, and heat losses during DW formation events, and we study their influence on large scale dynamics of the Adriatic basin. Many of the processes studied in this paper were already described in the literature, whereas our work aims to quantify them and estimate their variability. The primary goals of this study are, therefore, to explore the differences in available atmospheric reanalyses; to explore the sensitivity of Adriatic thermohaline properties and circulation to river runoff and atmospheric forcing; to understand the processes that govern the response of the Adriatic to changes in freshwater balance and to evaluate the main features of Adriatic circulation, such as DW formation and water exchange with the Mediterranean Sea. All of these findings should prove valuable in future modeling studies and contribute to a better understanding of the Adriatic system and its future in light of expected climate change.

We performed seven long term simulations of the Adriatic Sea with different atmospheric forcings and river discharge configurations. We used a medium-resolution CROCO ocean model known for its time-stepping efficiency (Soufflet et al., 2016). This allowed us to perform a large number of runs with relatively modest computer resources. Most of the pre and post-processing was done with the help of ROMSTOOLS/CROCO_TOOLS package (Penven et al., 2008). To improve the accuracy of our model, we recompiled the climatology of Albanian rivers with a new monthly runoff of Seman, Buna, and Drin.

2. Model Configuration

2.1. Rivers

A total of 43 freshwater sources were included in our model (Figure 1). The temperature of each source was set to the climatological temperature of the nearest available point in the World Ocean Atlas (WOA) climatology (NODC, 2009). Each of the sources was introduced through a dedicated channel with a length of several grid points, which ensured that the temperature of the discharge was adjusted to the air temperature before entering the basin.

We used measured monthly runoff for rivers Po (station Pontelagoscuro) (ARPAE, 2021), Isonzo (or Soča; station Solkan) (ARSO, 2020), and Rižana (station Dekani) (ARSO, 2020). For the other rivers, we used climatological monthly runoff - sourced from Vilibić et al. (2016) which is based on Raicich (1994) and Janeković et al. (2014). The locations of rivers are shown in Figure 1. We compiled a new climatology for some of the Albanian rivers. The climatological runoff of the rivers in the eastern part of the basin was modulated in accordance with the measured runoff of the Soča river and the climatological runoff of the rivers in the western part of the basin was modulated in accordance with a measured runoff of the river Po (Figure 2):

$$Q_n(t) = Q_{Cn}(m)\frac{Q_M(t)}{Q_C(m)} \quad (1)$$

Where Q_{Cn} is the climatological runoff for a given freshwater source at month m, Q_C is the climatological runoff of the reference river (Po or Isonzo) at month m, Q_M is the measured runoff of the reference river and Q_n is the runoff used in the model for the given freshwater source.

The use of Po and Isonzo as a reference for all the rivers of the Adriatic Sea is very far from the fact that real discharge data for each of the contributors would be necessary to achieve a highly realistic freshwater input. We

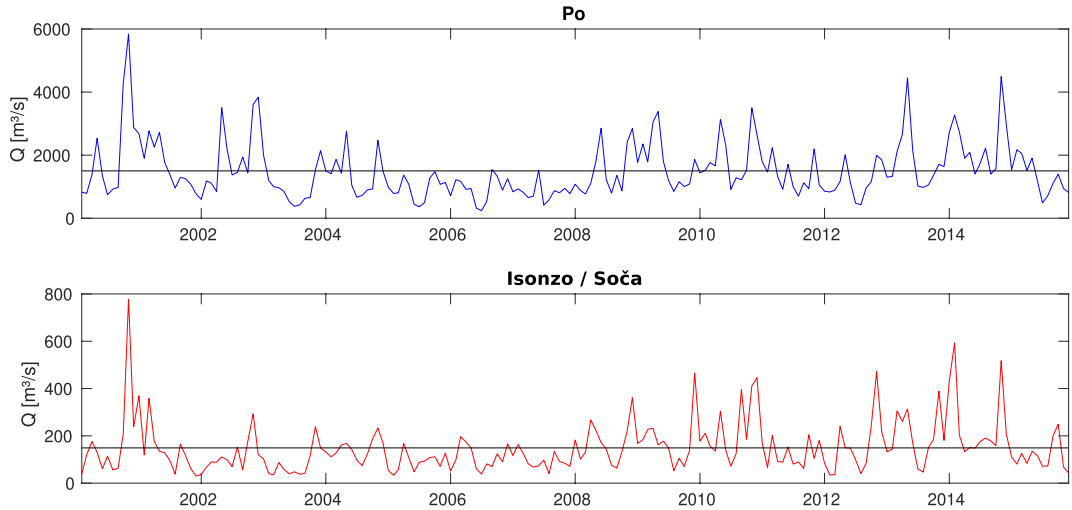

Figure 2. Monthly averaged runoff of Po and Isonzo (Soča) as used in the model runs. The black lines mark the 16-year average.

are aware of the dangers of using two Alpine rivers as modulators for the total Adriatic river discharge since the discharge in the south of the domain has little correlation with the rivers in the north. However, in this way, we introduced interannual variations to all freshwater sources in the model. Since this is a sensitivity study, such an approach introduces at least dry and wet years into the total discharge, rather than having the variations limited to the measured runoff only. The latter is about one-third of the total discharge, which amounts to 4,000 m^3/s on average throughout the simulation period.

As shown in the following chapters, our initial simulation with the described implementation of river runoff (baseline simulation - UERRA-B) resulted in a negative trend in salinity (Figure 8) and DW formation (Figure 10) and failed to reproduce the PDA saw-tooth pattern in the SAP (Figure 11). This is contrary to observations (Mihanović et al., 2013; Querin et al., 2016; Vilibić et al., 2019) and in order to test the sensitivity of the model to river runoff, we decided to run the simulations with reduced discharge, higher salinity of rivers, or both (Table 1). The higher river salinity runs ($S = 17$ for Po and $S = 15$ for other rivers) were performed in accordance with Verri et al. (2018) and Simoncelli et al. (2011). The prescribed salinity values are the result of sensitivity tests at locations of river mouths and at the center of the basin (Verri et al., 2018). The reduced runoff (DRY1 - 50% discharge of the baseline run) aims to better reproduce the observed salinity trends, and DW formation processes, while the extremely reduced runoff simulation (DRY2 - 20% discharge of the baseline run) is meant to represent extreme droughts which are expected to increase in frequency with the expected climate change.

2.1.1. Climatology of Albanian Rivers

A corrected runoff climatology has been compiled for three Albanian rivers: Buna, Drin, and Seman. The new climatologies are based on the 1981–2019 series of measurements from the Albanian National Hydrological Network. The water levels are measured 2 times in 24 hr (07 a.m. and 07 p.m.) and transformed into runoff with the Rating Curve method. Rating Curves are created using Current Meters or Doppler equipment to estimate the current speed at different water levels. Water level measurements from the last hydrological station before the river-mouth were obtained from the Institute of Geosciences, Department of Hydrology. The stations Mbrostar on Seman river (40°45,032' N, 19°34,654' E) and Dajç on Buna river (41°59,175' N, 19°24,850' E) are located about 20 km upstream from the river-mouth.

The new climatology raises the average outflow of Albanian rivers from 940 to 1,100 m^3/s (Figure 3), which makes these rivers a considerable freshwater source. For comparison, the most important tributary in the Adriatic Sea is river Po which contributes 1,500 m^3/s on average throughout our simulation period.

Table 1
River Runoff Configurations Used in the Simulations

	Discharge	Salinity
B	100%	1
DRY1	50%	1
DRY2	20%	1
SR	100%	17 (Po), 15 (other)
DRY1-SR	50%	17 (Po), 15 (other)

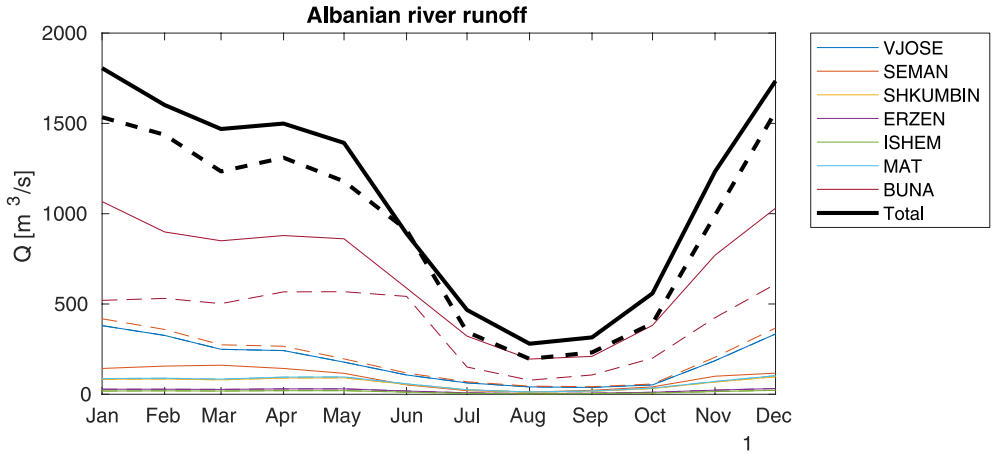

Figure 3. Monthly climatology of Albanian rivers. Dashed lines show the (Raicich, 1994) climatology, full lines show the updated climatological values.

While Rivers Vjose, Shkumbin, Erzen, Ishem, and Mat retain their runoff as studied by Raicich (1994), Seman's average outflow drops from 201 to 90 m^3/s. Rivers Buna (Bojana) and Drin have been merged into a single outflow channel. In the past, the paths of the Drin River and Buna River were separate. However, since the natural diversion of the River Drin some 150 years ago, the original channel of the Drin, leading south to the city of Lezha, carries only a relatively small discharge (renamed Drin i Lezhes). In 1956, it has been deviated artificially and the Drin flow now joins the Buna river just downstream of the Shkoder lake and continues as a single river along the border with Montenegro until it enters the Adriatic Sea. The new average outflow for Buna is 671 m^3/s, while in Raicich (1994)'s study on climatology, the contribution from Buna and Drin together was 400 m^3/s. The values used are listed in Table 2.

2.2. Atmospheric Products

The first atmospheric forcing dataset used in our experiments (marked as **UERRA**) is a combination of two products provided by the ECMWF. MESCAN-SURFEX is a high resolution two-dimensional surface analysis developed in the scope of the UERRA project (Bazile et al., 2017) and we combined it with ERA5 (Hersbach et al., 2020) shortwave and longwave flux. MESCAN-SURFEX is a downscaled product, based on the UERRA-HARMONIE 11 km atmospheric reanalysis on the European CORDEX EUR-11 domain (Giorgi et al., 2009; Niermann et al., 2018). The temperature at 2 m height, 10 m wind, relative humidity, and precipitation were provided with a 5.5 km horizontal resolution (Soci et al., 2016). Daily values were obtained from hourly values which were downloaded from ECMWF's Meteorological Archival and Retrieval System (ECMWF, 2021) and averaged over 24 hr. The high spatial resolution of MESCAN-SURFEX makes it a promising candidate for our purposes (Bertotti & Cavaleri, 2009; Signell et al., 2005). As this dataset lacks heat flux data, the latter were sourced from ERA5 with a lower spatial resolution (≃27 km).

We chose **ERA5** (Hersbach et al., 2020) as the second source of atmospheric forcing. ERA5 and its precursor ERA-Interim have become a de facto standard due to advanced physics, 4D-var data assimilation, and demonstrated high level of accuracy. Even though its 0.25° horizontal resolution is relatively coarse (≃27 km) considering the size of our model domain, it should be mostly bias-free and robust. Hourly values were downloaded from the Copernicus Climate Data Store (Hersbach et al., 2019) and averaged over 24 hr.

Table 2
Monthly Climatological Runoff [m^3/s] for Albanian Rivers That Differ From the Study by Raicich (1994)

River	January	February	March	April	May	June	July	August	September	October	November	December
Seman	143	156	161	143	116	52	20	12	22	41	100	117
Buna + Drin	1067	899	850	879	861	588	322	195	210	382	770	1030

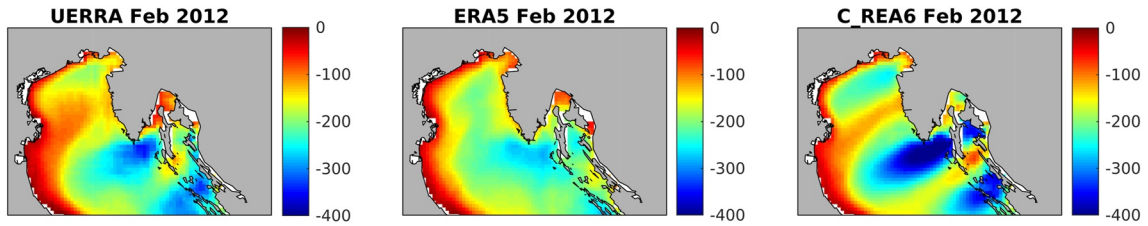

Figure 4. Average heat loss north of 44°N in February 2012 (in W/m^2). From left to right: UERRA-SR, ERA5-SR, and C_REA6-SR.

The third forcing dataset was derived from COSMO_REA6 reanalysis (marked as **C_REA6**). The latter is based on the COSMO model (Doms & Schättler, 2002), and its sister COSMO_REA12 ensemble reanalysis was part of the UERRA project as well. It covers the same CORDEX EUR-11 domain (Giorgi et al., 2009) as MESCAN-SURFEX, but in a 6 km spatial resolution. The results are available in hourly time-steps from 1995 to 2018. The boundary conditions for COSMO_REA6 were provided by ERA-Interim (Dee et al., 2011). Balloon ascents, aircraft reports, surface-level observations, and ship reports were assimilated using nudging data assimilation scheme (Bollmeyer et al., 2015). Daily averages were downloaded from the Deutsche Wetterdienst's data server (HErZ, 2021) for all variables except the wind. As average daily wind speed was not available, hourly values of U and V components were downloaded and averaged over 24 hr.

All the forcing fields were interpolated to the CROCO model grid using linear interpolation and packed into CROCO bulk forcing NetCDF files (Rew & Davis, 1990) using the ROMSTOOLS/CROCO_TOOLS package (Penven et al., 2008). All the fields, except for the wind, were masked with the land-sea mask and then extrapolated using the nearest neighbor method to dry grid-cells on their native grid. This ensured that only values calculated over the sea were used. The wind was not masked to prevent divergences in extrapolated values, especially between islands.

2.2.1. Wind

With steep orography along its eastern coastline and numerous islands, the circulation models of the Adriatic Sea should benefit from the improved horizontal resolution of atmospheric models (Bertotti & Cavaleri, 2009; Signell et al., 2005; Vilibić et al., 2016). These should offer a significantly better representation of wind patterns and speed. The model resolution should be particularly important in bora events (Janeković et al., 2014; Ličer et al., 2016), but is beneficial in sirocco ('jugo'; SE wind) events as well (Cavaleri & Bertotti, 1997). Bora is a NE cold and dry wind which blows through the gaps in the Dinaric Alps on the eastern part of the basin and forms well known strong jets (Ličer et al., 2016).

As expected, the atmospheric model with the highest horizontal resolution (COSMO_REA6) produces more pronounced bora jets (Figure 4). The average heat loss in February 2012, the month of the extreme DW formation event, shows significant differences between the models. This has considerable consequences on DW formation which will be shown to greatly influence the hydrology and circulation of the basin.

Daily measured and modeled wind speed at the location of the Vida buoy (Malačič, 2019) is shown in Figure 5. Vida is located in the Gulf of Trieste (GT), 2.2 km offshore (45°32.925' N, 13°33.042' E; Figure 1). The wind was measured in 30 min intervals and averaged over 24 hr. The modeled wind was taken from the bulk forcing files, from a grid point that was at least two grid cells from the land-mask to reduce the distortion of the wind field, and still close enough (45°34.392' N, 13°27.000') to the location of the buoy to be representative. In the left plot, we can see that COSMO_REA6 produces a much more realistic wind speed during the extreme bora event in 2012 (RMSE = 1.6 m/s), while UERRA and ERA5 both underestimate the wind speed during the event (RMSE = 4.6 and 4.8 m/s, respectively). It is somewhat surprising that UERRA only slightly outperforms ERA5 even though its horizontal resolution is much higher (Table 3). In the right plot in Figure 5 UERRA (R = 0.93, RMSE = 1.5 m/s) outperforms both ERA5 (R = 0.71, RMSE = 2.4 m/s) and COSMO_REA6 (R = 0.92, RMSE = 1.6 m/s). UERRA's advantage over the former is expected due to higher spatial resolution, but over the latter not so much. However, we can see, that COSMO_REA6 outperforms the other two in strong winds (as was the case in the bora 2012 event), but on the other hand, it underestimates the wind speed in low wind conditions (below 7 m/s).

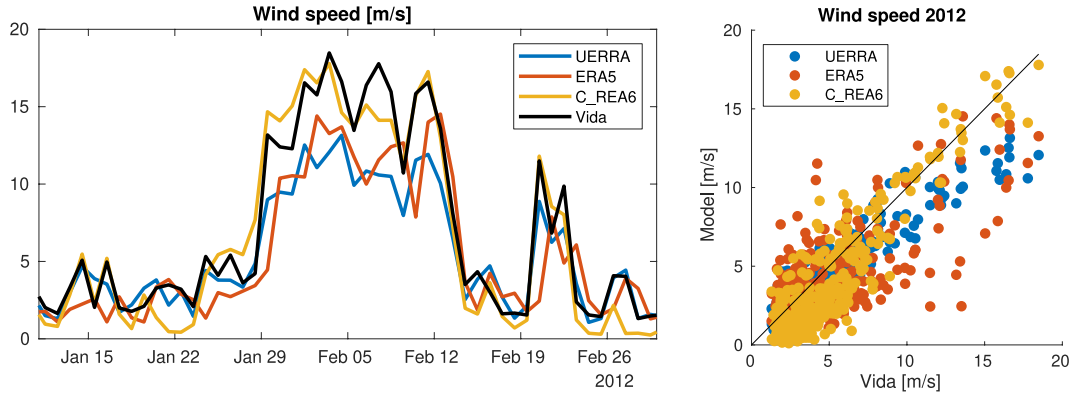

Figure 5. Left: Measured and modeled daily averaged wind speed at Vida oceanographic buoy during the 2012 extreme bora ('burja') event. Right: scatter plot of measured versus modeled wind speed at the location of the Vida oceanographic buoy for the year 2012.

2.2.2. Evaporation–Precipitation

The surface freshwater flux or evaporation minus precipitation (E–P) differs significantly, depending on the atmospheric model used to provide the surface boundary conditions (Figure 6 and Table 4). The evaporation-precipitation budget was calculated over the wet cells (sea) in our model domain. The evaporation is calculated by the CROCO ocean model via a bulk formula (Fairall et al., 1996), while the precipitation is obtained from the atmospheric model, interpolated to the model grid, and limited to the wet part of the domain only. The budget for each cell is calculated and averaged for each month by the CROCO ocean model during runtime. The differences in total surface time averaged freshwater flux, shown in Table 4, are of the same order of magnitude as the variations in river runoff and should have a significant influence on the salinity of surface waters at least.

2.3. The Ocean Model

We used Coastal and Regional Ocean COmmunity model (CROCO v1.1 ocean model, formerly known as ROMS_AGRIF; www.croco-ocean.org) which is a branch of Regional Ocean Modeling System. The horizontal resolution was set to 4 km, the vertical discretization consisted of 32 sigma levels. Bathymetry smoothing was performed using the 'LP volume method' (Sikirić et al., 2009) to keep the configuration as realistic as possible while reducing the internal pressure gradient error (Berntsen & Oey, 2010). The Fairall (Fairall et al., 2003) bulk formula was used for atmospheric forcing, while a combination of characteristic and Orlanski conditions was used at the open boundary - the default CROCO setting.

Initial and boundary conditions were obtained from Med MFC physical reanalysis (Escudier et al., 2020), a product provided by the MFS modeling system (Pinardi et al., 2003). The product is based on the NEMO code (Madec & Team, 2022), with 1/24° horizontal resolution and 141 vertical Z-levels. Daily mean MFS values were used at the open boundary of our model, while the daily average for 1 January 2000 was used as the initial state.

Table 3
Model Configurations Used in the Analysis

tag.	Surface var.	Atm. resolution	Heat fluxes	River runoff
UERRA-B	MESCAN-SURFEX	27/5.5 km	ERA 5	100%, fresh
UERRA-SR	MESCAN-SURFEX	27/5.5 km	ERA 5	100%, salty
UERRA-DRY1	MESCAN-SURFEX	27/5.5 km	ERA 5	50%, fresh
UERRA-DRY2	MESCAN-SURFEX	27/5.5 km	ERA 5	20%, fresh
UERRA-DRY1-SR	MESCAN-SURFEX	27/5.5 km	ERA 5	50%, salty
ERA5-SR	ERA5	27 km	ERA 5	100%, salty
C_REA6-SR	COSMO_REA6	6 km	COSMO_REA6	100%, salty

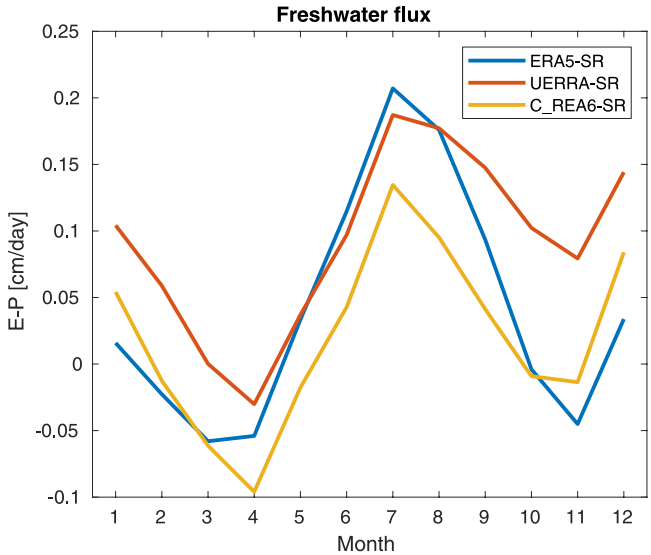

Figure 6. Monthly mean surface freshwater flux for different atmospheric products (E-P in cm/day), calculated using bulk formula (Fairall et al., 2003).

The model horizontal resolution was set at 4 km and was chosen to be fine enough to suit the resolution of the atmospheric forcing while being coarse enough to run on a regular personal computer with 8 computing cores (HP ZBook, Intel I9 processor, 32 GB of RAM).

3. Results

3.1. Vertical Profiles

Time and depth averaged salinities are shown in Figure 7. The model runs are averaged over the 2006–2015 period and compared to MEDAR (MEDAR Group, 2003) and SeaDataNet (www.seadatanet.org) Mediterranean Sea climatologies. After the intensive 2006 DW formation event, the water from the initial state has been replaced through the entire water column and therefore the water properties are indicative of the model configuration and its performance. The climatological profiles in Figure 7 differ significantly in the top 50 m but tend to match better with the low salinity runs. In the mid-depths (150–500 m) the climatological salinity is quite constant and matches best with saltier runs. The low salinity runs show an increase in salinity with depth, while the UERRA-DRY2 and UERRA-DRY1-SR are rather constant. The climatologies exhibit a slight drop in salinity below 700 m (close to the depth of Otranto sill) and the same is very pronounced in C_REA6, but can be observed in other low salinity runs as well. C_REA6 is fresher than the climatologies at the bottom of the basin, while the other runs are somewhat saltier.

3.2. Water Circulation

The model results reveal an intricate interplay of several processes that significantly influence the water exchange between the shelf, the bottom of the Southern Adriatic Pit (SAP), the Southern Adriatic, and the Mediterranean Sea. The salinity of the surface waters in combination with heat losses during strong wind events seems to play a decisive role in this self-amplifying loop. The mechanism will be described in the following sub-sections along with the model results.

3.2.1. Adriatic Shelf (Northern and Central Adriatic Sea)

Volume averaged salinity of the water north of the Palagruža sill (Figure 1) is shown in Figure 8. Due to shallow topography and considerable river discharge in this area, the salinity of the shelf water is strongly influenced by river runoff (especially Po runoff) and the surface freshwater flux as well. The latter claim is supported by a noticeable difference in salinity between UERRA-SR, ERA5-SR, and C_REA6-SR runs. These runs differ only in atmospheric forcing, so the differences in averaged shelf salinity in Figure 8 can be attributed to differences in E-P. The UERRA-B, ERA5-SR, and C_REA6-SR runs produce markedly fresher shelf water and the average salinity falls bellow the initial value. This indicates that the total freshwater input is overestimated in these configurations (assuming the initial value, obtained from the Med MFC, is realistic). On the other hand, the UERRA-DRY2 and UERRA-DRY1-SR run quickly rise above initial average salinity and never drop below that value, and likely the total freshwater input is underestimated.

Table 4
Time Averaged (2000–2015) Evaporation Minus Precipitation for Different Atmospheric Forcing

Model	E-P [m^3/s]
ERA5	808
UERRA	1401
COSMO_REA6	380

Dense Water Formation: The salinity of the surface layers is an important factor in the DW formation process and this is reflected in the total volume of DW in the Adriatic basin (Figure 9) and in the flow of DW over the Palagruža sill toward the SAP (Figure 10). Unsurprisingly the runs with saltier freshwater balance produce larger peaks in DW volume and larger flow of DW from the shelf toward the SAP.

Pronounced peaks in DW transport south can be observed in 2012 (Figure 10), which coincides with a now famous DW formation event, but are surpassed

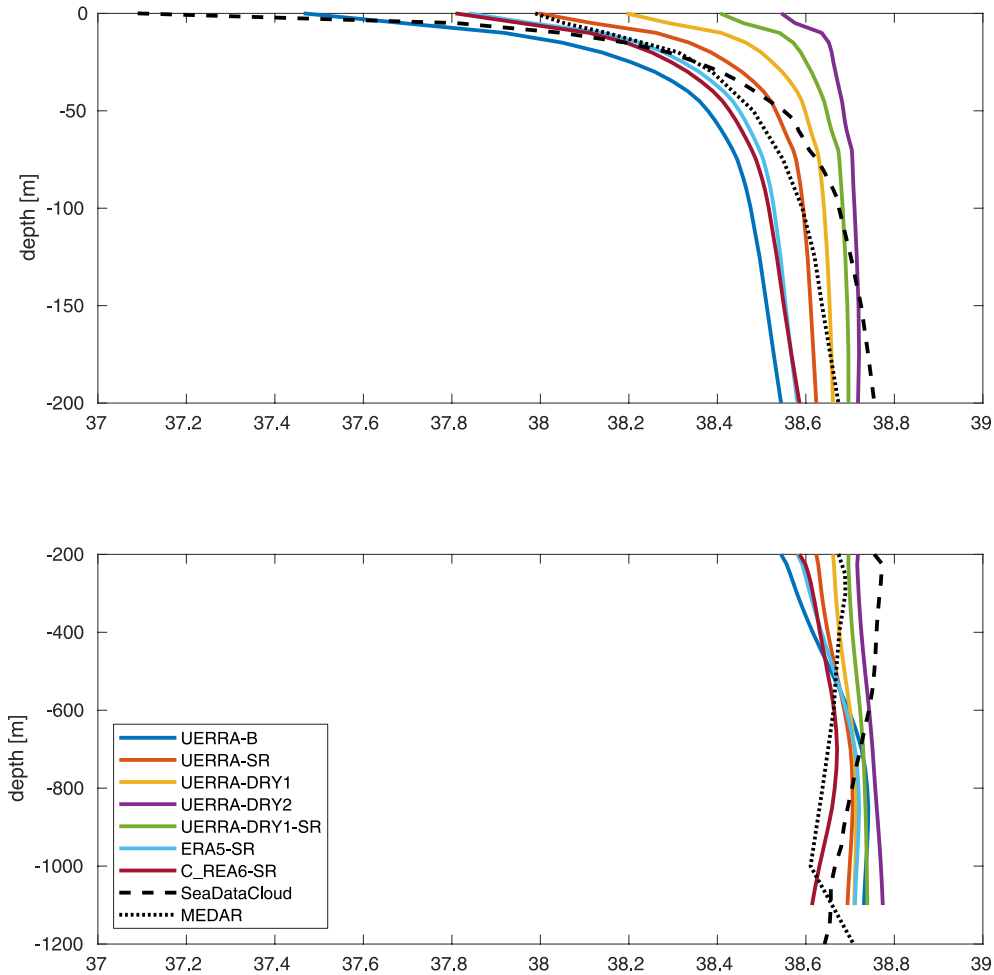

Figure 7. Salinity - time and area averaged over the whole model domain. Model runs compared with SeaDataCloud and MEDAR climatologies (see Open Research section). The model runs are averaged over 2006–2015 period.

by the DW formation in 2006. Although the latter was less intensive from the meteorological perspective, it produced a larger volume of DW although of lower density. The 2012 event featured higher wind speeds but was confined to a smaller area.

The C_REA6-SR produces very high amounts of DW (Figures 10 and 9) even though it has a relatively fresh freshwater balance (Table 4) and low average salinity (Figure 8). These high volumes of DW production are a consequence of higher heat losses (Figure 4), so the produced DW is fresher and colder than in the other runs (Figure 11 and next section).

3.2.2. Southern Adriatic Pit (SAP)

As shown by Querin et al. (2013), the DW that forms on the shelf travels southward as a bottom density current that passes the SAP on it's western flank. The densest DW separates from this flow and enters the deeper layers of the pit, while lower-density DW flows further south toward the Strait of Otranto and then into the Ionian Sea.

DW inflow events in our simulations can be clearly seen in both plots in Figure 11 which shows average salinity and PDA at the bottom layers of the SAP (below 800 m depth). The PDA plot (bottom) exhibits the saw-tooth pattern produced by jumps in density caused by the inflow of fresh DW as described in Querin et al. (2016). The saw tooth pattern is clearly visible for the UERRA-DRY1, UERRA-DRY2, UERRA-SR, and UERRA-DRY1-SR run while no such pattern can be observed for UERRA-B and ERA5-SR runs. The latter two exhibit changes in salinity caused by DW inflow, which are visible in the top plot. But these two runs have the lowest shelf salinity (Figure 8) and produce DW that is not dense enough to interrupt the decrease in PDA. The gradual density

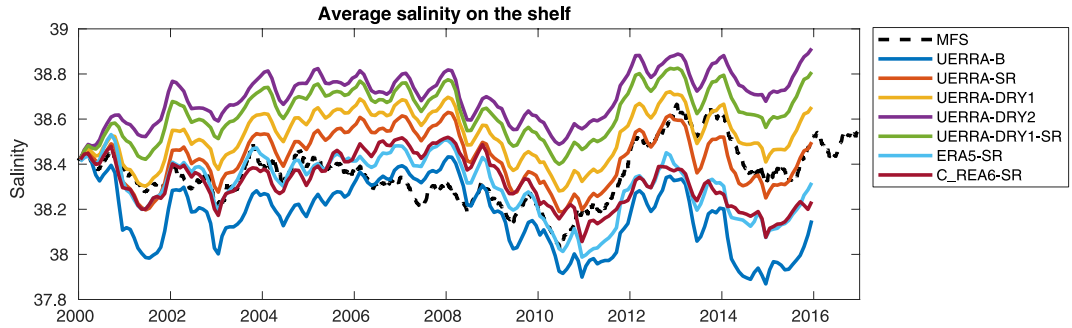

Figure 8. Volume averaged shelf (north of Palagruža sill - Figure 1) salinity. Model runs can be compared with the MFS (dashed black line).

decrease was observed in measurements and explained by mixing of the bottom DW with warmer and less dense inflowing Mediterranean water (Querin et al., 2016).

C_REA6-SR produces the largest salinity drop (Figure 11), while PDA is similar to UERRA-DRY1, meaning that the DW formed in C_REA6-SR is colder than in the other runs. This is explained by the higher spatial resolution of atmospheric forcing which produces local peaks of heat loss (Figure 4). C_REA6-SR also has the lowest E-P of all atmospheric models in our experiment, which results in low salinity of surface layers.

The surprising feature in Figure 11 is that the UERRA-DRY1 and UERRA-SR runs feature fresher water in the SAP than the baseline UERRA-B run. The shelf salinity of UERRA-DRY1 and UERRA-SR runs is higher than in UERRA-B (Figure 8) and the resulting DW is saltier. The unusual salinity of SAP deep layers can be explained by the fact that the DW formed in these saltier runs is still fresher than the Mediterranean water coming through the Strait of Otranto, while the volume of this DW is several times larger than in the UERRA-B run (Figure 10). Therefore, increased salinity of shelf water actually causes a decrease in salinity of the bottom layers of the SAP as a consequence of increased DW inflow. However, in the UERRA-DRY2 and UERRA-DRY1-SR runs, the DW inflow events cause an increase in salinity in the SAP. In these two extreme cases (one with runoff reduced to 20% and the other with halved runoff and increased salinity) the salinity of the shelf water (Figure 8) often exceeds the salinity of the inflowing Mediterranean water ($S > 83.7$, Figure 16) and the newly formed DW that is filling the SAP is saltier than the water already in the pit, producing upward jumps in the salinity of bottom layers.

3.2.3. Adriatic Meridional Overturning Circulation (AdriMOC) and the Water Exchange Through the Strait of Otranto

The work by Cessi et al. (2014) and Verri et al. (2018) shows that the buoyancy flux in adjacent seas such as the Adriatic could control the meridional overturning circulation toward estuarine (freshwater outflow in the top layer and an inflow of saltier water below) or anti-estuarine (reversed) dynamics. While Verri et al. (2018) study the whole Adriatic-Ionian system, our work focuses on the Adriatic Sea and the Strait of Otranto.

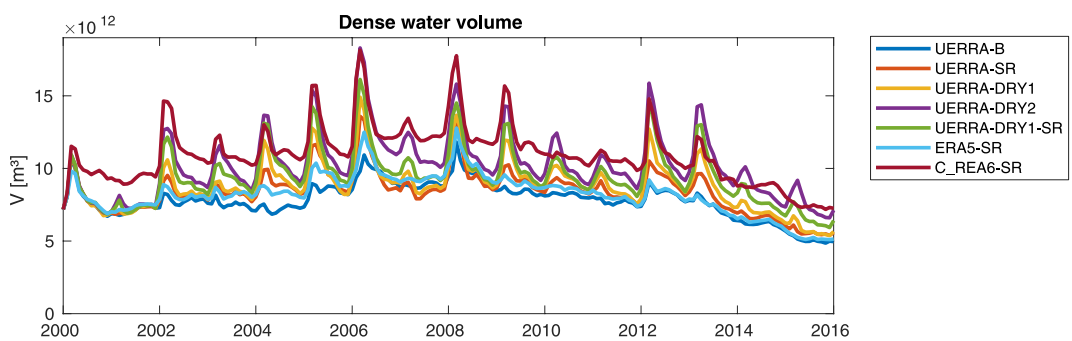

Figure 9. Volume of dense water ($PDA > 29.2$ kg/m³) in the Adriatic basin.

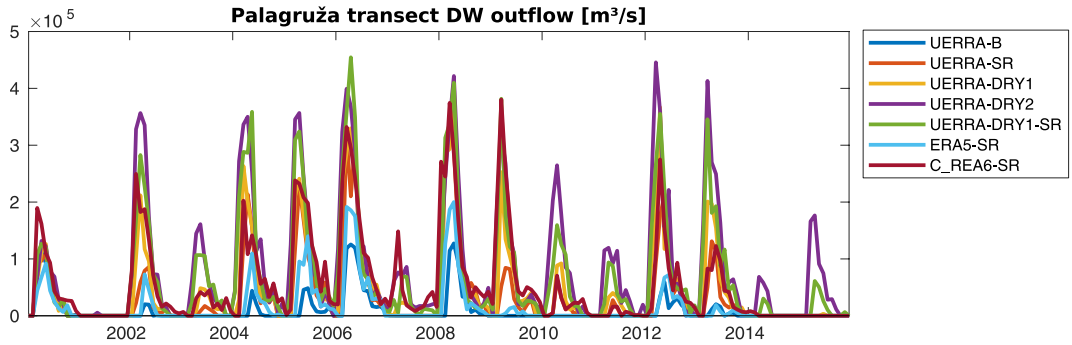

Figure 10. Outflow of dense water ($PDA > 29.2$ kg/m³) through the Palagruža transect (blue line in Figure 1).

Figure 12 shows the stream function computed on meridionally averaged velocity. We use the same equation as used in the study by Verri et al. (2018) who in turn followed Pedlosky (1987):

$$\Psi(y,z) = -\int_{x_o}^{x_1}\int_{-H}^{z} v(x,y,z)dxdz \tag{2}$$

Following Verri et al. (2018) we calculate the buoyancy flux per unit area (m^2 s^{-3}):

$$Q_b = \frac{g\alpha_T}{\rho_{0w}C_w}Q - \alpha_s S_0 g(E - P - R/A) \tag{3}$$

The first term on the right is the heat term, while the second is the sum of evaporation, precipitation, and runoff. The runoff part of the equation consists of river discharge (R; in m^3 s^{-1}) divided by the total surface area of wet cells in the model (A; in contrast to Verri et al. (2018) who use the grid area of river mouths). The following constants are used: g - gravitational acceleration (9.8 m s^{-2}); α_T - coef. of thermal expansion ($2.3 \cdot 10^{-4}$ K^{-1}); α_s coef. of haline expansion ($7.5 \cdot 10^{-4}$); ρ_{0w} - reference water density (1,029 kg m^{-1}); C_w - sea water heat capacity (3,990 J kg^{-1} K^{-1}); S_0 surface salinity (38.7). The total Q_b for all the runs for the 2000–2015 period is shown in Table 5.

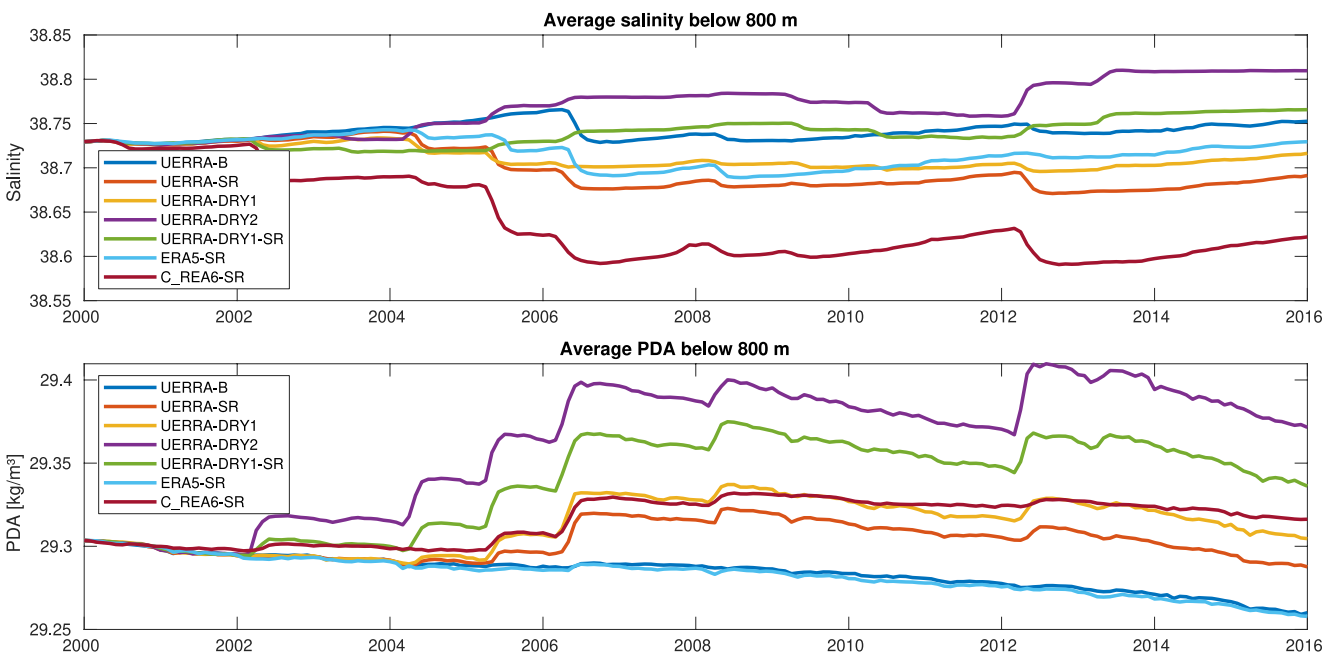

Figure 11. Average salinity (top) and potential density anomaly (bottom) for the deepest part of the SAP ($H > 800$ m - below the Otranto sill).

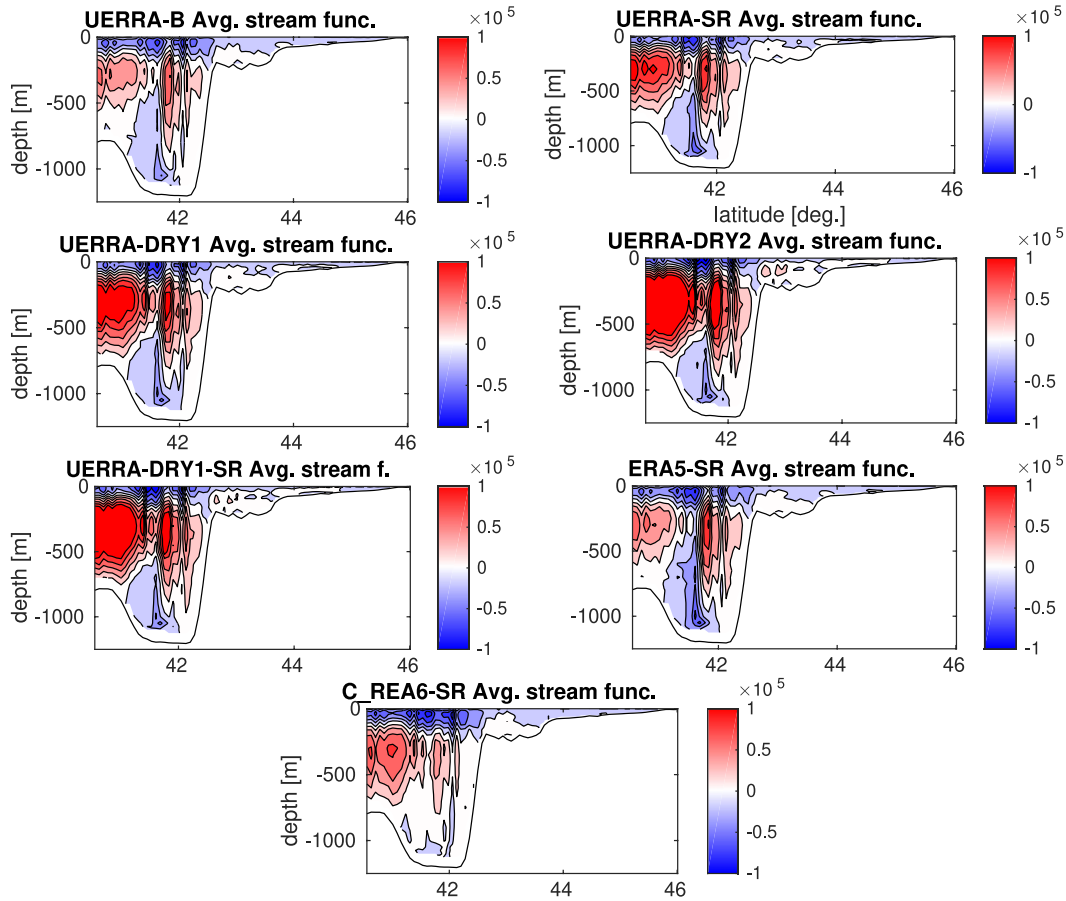

Figure 12. Average transport stream function (in m^3/s) for the 2001–2015 period. Latitude in degrees is plotted on the *x* axis.

In contrast to Verri et al. (2018), the baseline (UERRA-B) and salty rivers run (UERRA-SR, ERA5-SR, C_REA6-SR) demonstrate positive average buoyancy flux, which turns to negative values only in the runs with reduced runoff. This is likely a consequence of the different surface areas used in the runoff term of the buoyancy flux Equation 3. Even though the runs with positive buoyancy should induce estuarine circulation, the main pattern is still anti-estuarine (Figure 12). The intensity of anti-estuarine cells is amplified with the reduction of river runoff as expected (UERRA-DRY1, UERRA-DRY2, UERRA-DRY1-SR).

Table 5
Time and Surface Averaged Buoyancy Flux for the 2000–2015 Period

Run name	Q_b [10^{-9} m^2 s^{-3}]	ΔQ_b [%]
UERRA-B	2.8	
UERRA-SR	0.80	−72
UERRA-DRY1	−4.0	−240
UERRA-DRY2	−7.7	−380
UERRA-DRY1-SR	−4.8	−270
ERA5-SR	4.1	46
C_REA6-SR	4.7	68

Note. The last column shows the change from the baseline simulation (UERRA-B).

The comparison between the yearly averaged buoyancy flux and the yearly averaged stream function difference between 400 m depth and surface at 41°N (Figure 13) indicates there is little to no correlation between the two on the yearly level. Indeed, the correlation coefficient spans from −0.14 for the C_REA6-SR run to 0.2 for the UERRA-B. On the other hand, Figure 14 shows clear peaks in stream function difference in the years with intensive DW formation. The latter was identified by the peaks in total DW volume (Figure 9). Looking at Figure 14 it is therefore unsurprising that the correlation coefficient between the yearly averaged DW outflow through the Otranto Strait and the yearly averaged stream function difference exhibits much higher values (from 0.77 for ERA5-SR to 0.93 for UERRA-DRY1-SR).

The influence of DW formation on the meridional overturning circulation explains the surprising behavior of the C_REA6-SR stream function. Although it has the highest average buoyancy flux (Table 5 and Figure 13), it does not produces the weakest anti-estuarine circulation (Figures 12 and 13).

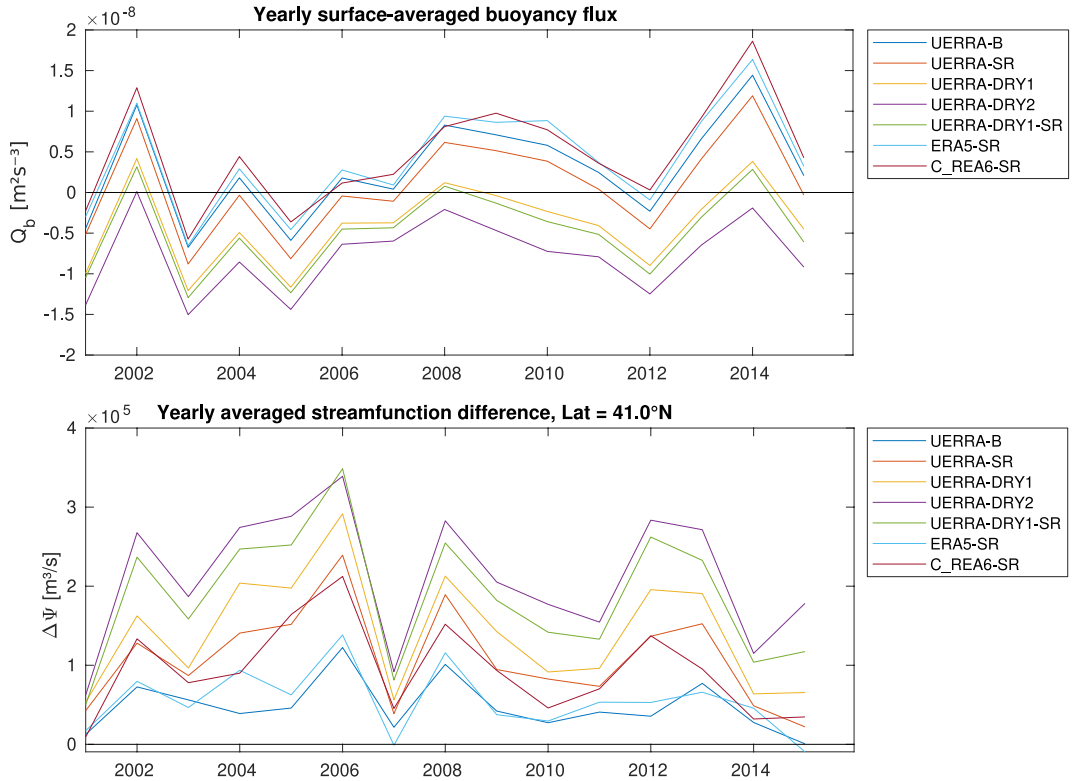

Figure 13. Yearly averaged buoyancy flux (top) and Yearly averaged streamfunction difference between surface and 400 m depth at 41°N (bottom).

This is explained by large DW production in this model configuration which amplifies the anti-estuarine character of the circulation in C_REA6-SR.

The Strait of Otranto: In Figure 15 we plot the W-E transect at the shallowest part of the strait (40.7°N) for April 2012 which is about 2 months after the very intensive DW formation event. The dashed line marks the PDA of 29.2 kg/m^3 and the plots clearly demonstrate that the runs with saltier freshwater balance, produce a much larger outflow of DW through the strait. The dotted line marks the salinity of 38.7 and we can see that the same runs produce a higher inflow of salty Mediterranean water as well. On the right-hand side of the figure, a rise of the isopycnals toward the surface can be observed. This allows for a larger inflow of salty water (due to a larger transect area) and its placement into shallower layers of the Adriatic Sea. The latter is important in the intrusions of the Mediterranean and modified Mediterranean water to the shelf (next section). Furthermore, the current speeds are larger in the runs with higher surface salinity. The flow is horizontally separated in the UERRA-B run, while

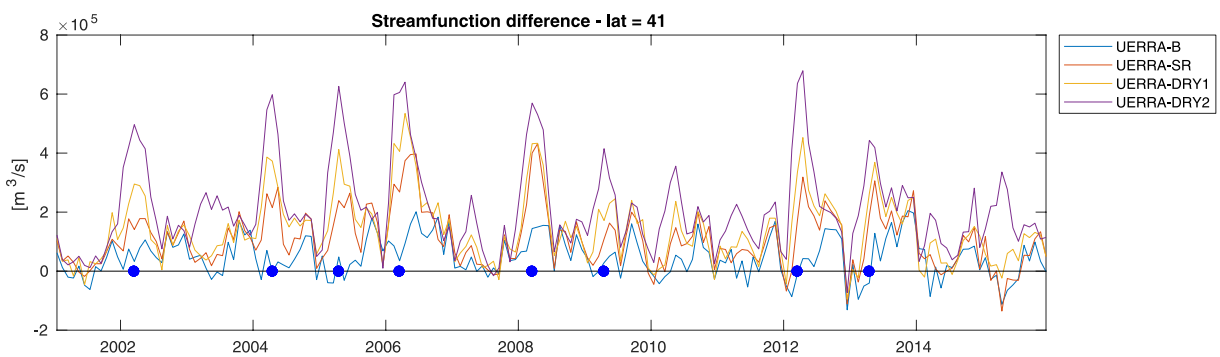

Figure 14. Stream function difference between 400 m depth and surface at 41°N. Blue dots mark intensive DW formation events (see Figure 9) and Figure 16.

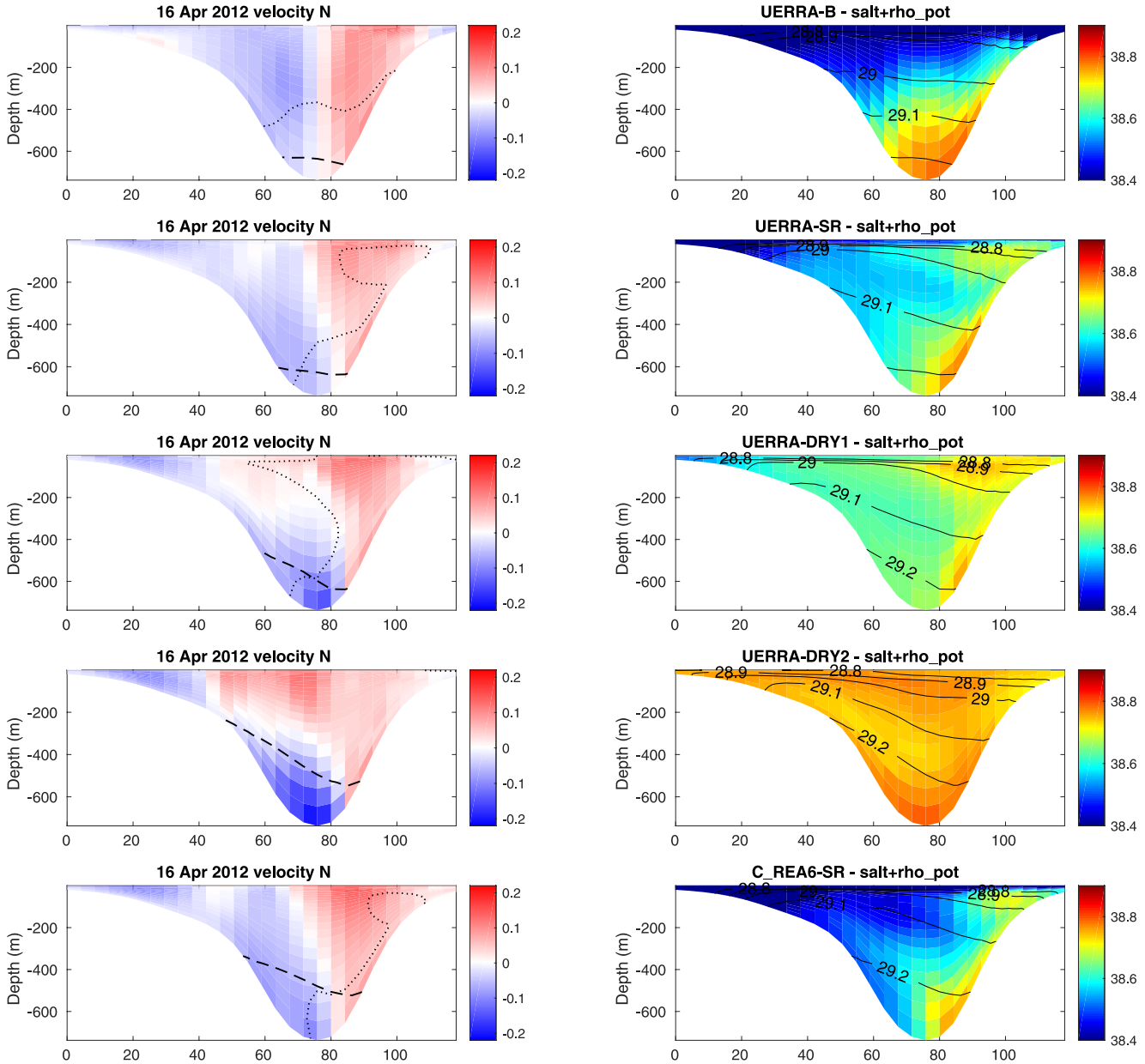

Figure 15. Otranto transect (40.7°N, see Figure 1), average values for April 2012. The *x* axis shows the position along the transect in km. Left: velocity is in m/s, dashed line marks DW ($PDA > 29.2$ kg/m³) and dotted line marks salty Mediterranean water ($S > 38.7$). Right: Salinity in color, lines show potential density anomaly in kg/m^3.

the separation is semi-vertical in the UERRA-DRY2 run. This additionally explains why the latter exhibits a much stronger anti-estuarine stream function than the former.

The transport of DW ($PDA > 29.2$ kg/m^3) through the Strait of Otranto is shown in Figure 16. Looking at UERRA-based runs we can again observe that the runs with saltier freshwater balance export a larger amount of DW to the Ionian Sea.

Table 6
Time Averaged Dense Water Outflow Through Otranto Strait and Palagruža Transect

Run name	Palaguža [10^3 m^3/s]	Δ [%]	Otranto [10^3 m^3/s]	Δ [%]
UERRA-B	9	0	34	0
UERRA-SR	34	230	71	110
UERRA-DRY1	47	360	100	200
UERRA-DRY2	84	720	190	460
UERRA-DRY1-SR	68	560	150	340
ERA5-SR	16	56	39	14
C_REA6-SR	57	450	140	310

4. Discussion

4.1. Water Exchange

The amount of DW exiting the Adriatic Sea is 2–4 times the outflow at Palagruža transect (Figure 10 and Table 6) and we can conclude that the amount of DW formed by deep convection in the southern Adriatic is about 1–3 times the amount of DW that forms on the shelf. However, the shelf DW (SDW) production might be underestimated due to the relatively low horizontal resolution of our model which is likely inadequate to properly resolve the water dynamics in the Kvarner Bay (Figure 1 - KV) and due to low temporal resolution of atmospheric forcing (daily averages). Comparing the DW outflow and Mediterranean salty water ($S > 38.7$) inflow (Figure 16), we can confirm that the runs with higher surface salinity not only export larger volumes of DW but also import significantly larger amounts of salty Mediterranean water into the Adriatic basin. The exception here is C_REA6-SR with a rather low surface salinity, large DW production, and relatively modest import of Mediterranean salty water. The first is a consequence of very low E-P, the second is a result of intensive heat losses during high wind events and the third is caused by the overall freshening of the upper layers of the basin.

Looking at the DW import in Figure 16, we can observe that peaks of inflow follow DW export events and often also precede them. This is in line with the claim that preconditioning is essential to ensure larger volumes of DW production (Mihanović et al., 2019). The inflow of salty water declined from 2009 onward and started recovering in 2011, which matches the period of anticyclonic BiOS regime in the Ionian sea, with a 1 to 2-year delay (Denamiel, Tojčić, Pranić, & Vilibić, 2022). The latter lasts from 2008 to 2010 and changes the source of inflowing Mediterranean water from very salty Levantine to modified Atlantic water which is fresher (Mihanović et al., 2021).

The yearly averaged total inflow through the Strait of Otranto (Figure 17) confirms that the DW formation has a significant impact on the water exchange between the Mediterranean and the Adriatic Sea and does not seem to be affected by changes in Ekman transport. The decrease in inflow can consistently be observed in years with no DW formation. The low salinity run UERRA-B features a drop in inflow in 2002 as well, despite it being a DW formation year. This is likely a consequence of adjustment from initial conditions to new salinity balance in the basin.

Our results show that the inflow/outflow regime through the Strait of Otranto alternates between vertically and horizontally separated flow (Figure 15). The DW outflow at the bottom of the strait induces vertically separated water exchange, while in the periods of low DW outflow the exchange flow is primarily separated horizontally.

Our modulation of the climatological runoff with the measured values for Po and Isonzo helped us to introduce interannual variations in river discharge. This is a kind of first-order correction for the monthly climatological values, although the difference between the actual monthly discharge and our approximation is still likely to be quite significant for many of the rivers. However, our approach ensures a more realistic reduction in freshwater inflow during drought years (e.g., 2003; Poulain et al. [2004]) and should ensure a more realistic DW production and reproduction of high salinity events (Mihanović et al., 2021). Establishing a realistic freshwater discharge budget is a daunting task due to a large number of rivers, as well as many underwater springs and small contributors. As we are more interested in the main processes and sensitivity of the system, adding more complexity to river runoff would not change the main conclusions of this study.

The high interannual variability (Cozzi & Giani, 2011) of the river runoff limits the usefulness of runoff climatologies in many applications (e.g., forecasting). Given the relative uncertainties in the discharge of many Adriatic rivers and the large differences in the surface freshwater flux, it may be beneficial to run multiple model configurations as an ensemble to ensure that all processes are properly represented.

4.2. Back to the Shelf: Salt Water Intrusions

The saltier shallow layers in the southern Adriatic and intensified water exchange through the Strait of Otranto produce more salty water (Mediterranean and modified Mediterranean water) intrusions to the shelf (Figure 18). These intrusions are important in preconditioning the DW formation (Mihanović et al., 2019) and the extreme

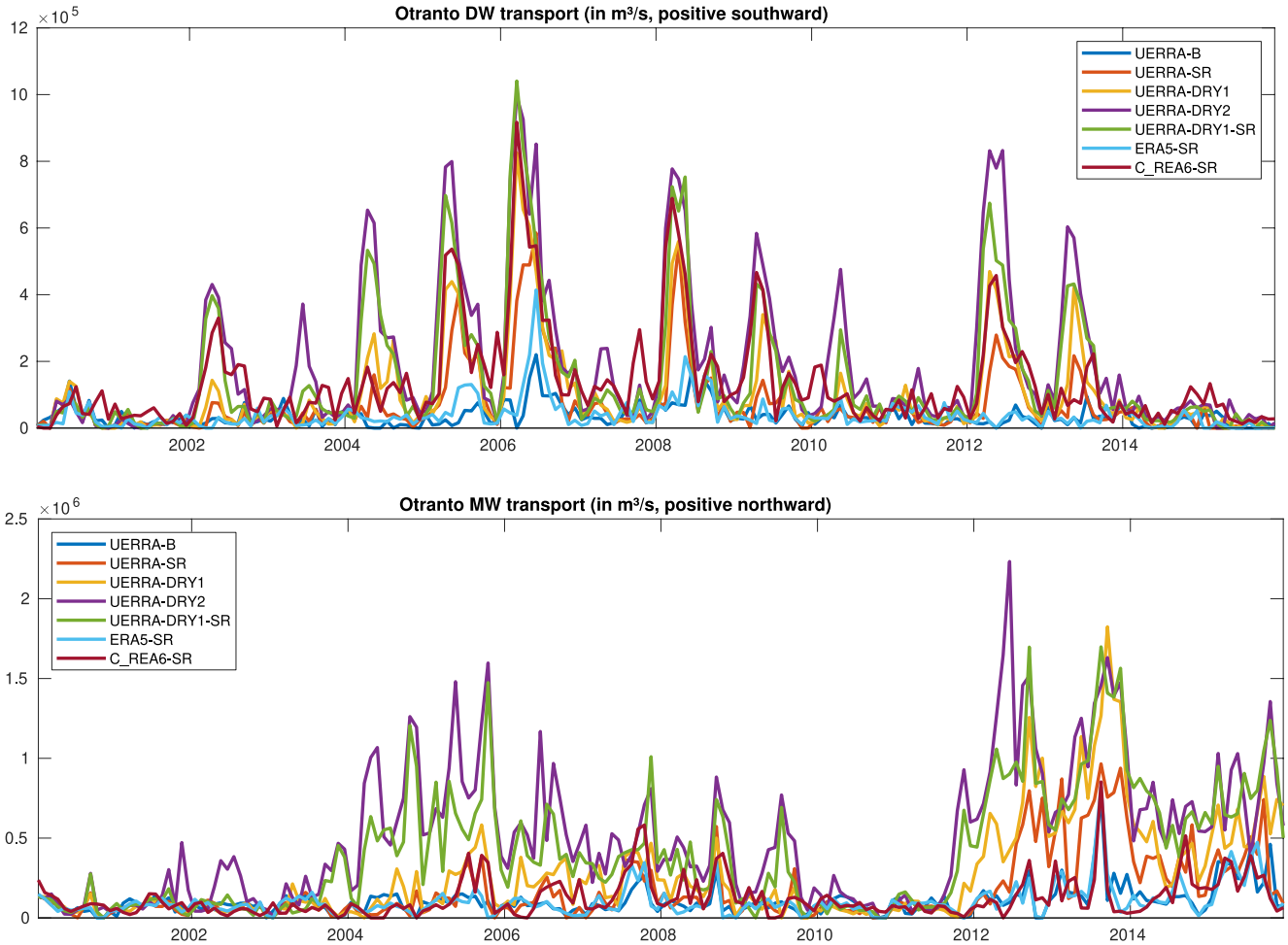

Figure 16. Outflow (top) of DW ($PDA > 29.2$ kg/m^3) and inflow (bottom) of salty Mediterranean water (MW; $S > 38.7$; bottom) through the Strait of Otranto (transect at 40.7°N).

salinity events as described in Mihanović et al. (2021). They are also the last component of the salinity loop as they make the shelf water even saltier amplifying the effects of reduced river runoff and evaporation. The salinity rises even more and this in turn favors even more intensive DW formation.

4.3. Atmospheric Forcing

The results of our simulations show that the choice of atmospheric forcing significantly affects the freshwater balance in the basin (Table 4 and Figure 8) and greatly affects the DW production (Table 6, Figures 10 and 16). The consequences of the chosen atmospheric forcing can be felt through the entire water column down to the bottom of the SAP (Figure 11).

At this point, we are able to explain the unusual properties of the C_REA6-SR run. Although it has the lowest precipitation and evaporation balance of all three SR runs (UERRA-SR, ERA5-SR, C_REA6-SR), the volume-averaged salinity on the shelf surpasses that of ERA5-SR most of the time (Figure 8). Although the freshwater balance is fresher than in the other two SR runs, the heat losses during DW formation events are so large that it produces larger DW outflow through the Palaguža transect (Figure 10) and the Strait of Otranto as well (Figure 16). Furthermore, it results in the largest volume of DW in the basin (Figure 9) and that includes all the runs, including those with extremely salty freshwater balance. It also produces the lowest salinity of the water at the bottom of the SAP (Figure 11). Therefore, the C_REA6-SR exports a large amount of low-salinity water to the deep layers of the Adriatic Sea and that explains why the shelf salinity is higher than expected.

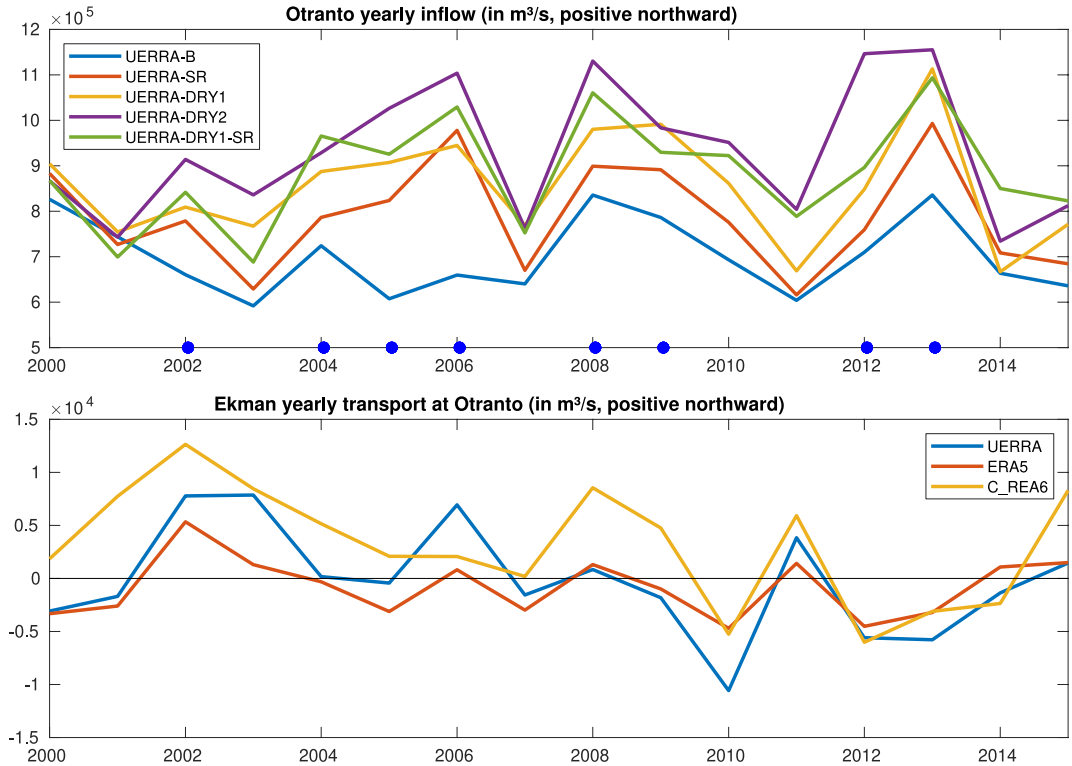

Figure 17. Yearly averaged water inflow (top) and Ekman transport (bottom) through the Strait of Otranto (transect at 40.7°N - Figure 1). The blue dots in the top plot indicate years with intensive DW formation.

As the results of C_REA6-SR show, the salinity of the surface layers does not depend only on the freshwater balance (runoff, evaporation, precipitation) but is indirectly influenced by heat losses during DW formation events as well.

4.4. Comparison With Previous Studies

Our work is similar in many ways to Dunić et al. (2019), but as the latter focuses on the model performance aspect, our interest lies primarily in the general circulation processes and their sensitivity to freshwater input and atmospheric boundary conditions. The DW volume obtained in their simulations matches well with our findings (Figure 9) and similarly to our results, most of the configurations in Dunić et al. (2019) exhibit negative salinity bias with the only exception being the atmosphere-ocean coupled models. This confirms our conclusions that the salinity of the basin depends on a delicate balance between river runoff and E-P provided by the atmospheric

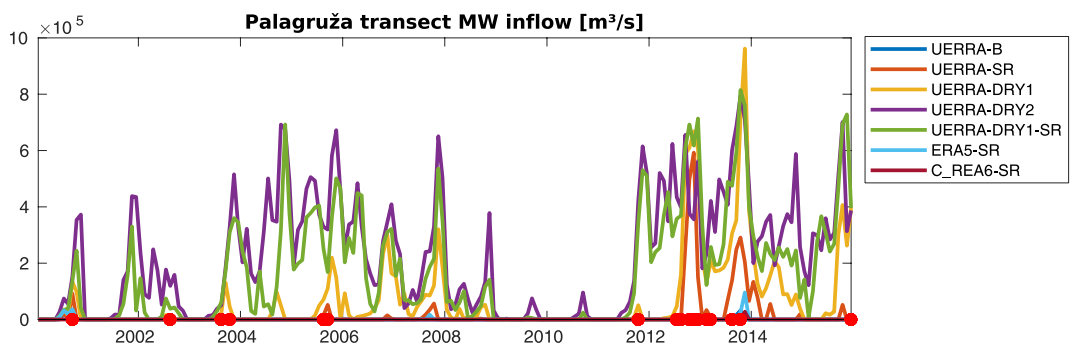

Figure 18. Inflow of salty Mediterranean water (MW; $S > 38.7$) through the Palagruža transect (blue line in Figure 1). Red dots mark the recorded exceptional salinity events (Mihanović et al., 2021).

Table 7
Volume of Dense Water (PDE > 29.2 kg/m³) Transported Through the Palagruža and Otranto Transects During January–August 2012

Run name	Palagruža [km³]	Otranto [km³]
UERRA-B	430	470
UERRA-SR	1,800	2,900
UERRA-DRY1	2,700	5,000
UERRA-DRY2	4,000	11,000
UERRA-DRY1-SR	3,200	7,800
ERA5-SR	620	570
C_REA6-SR	2,000	5,200

models. On the other hand, their study produced only minor changes in average thermohaline properties with the introduction of new river climatology (44 freshwater sources instead of 8). This is quite the opposite of our results which show high sensitivity to freshwater input, especially in DW formation and consequently SAP water properties and water exchange with the Mediterranean Sea.

ROMS + Aladin/HR atmosphere-ocean modeling system with several runoff configurations was used to test the DW production sensitivity to freshwater input in Vilibić et al. (2016). The atmospheric model ran at 8 km horizontal resolution with the wind downscaled to 2 km. They tested two river climatologies and a blend of climatological and measured river runoff to model the 2012 DW formation event. All of the runs produce lower salinity than observed in the two reference locations. The volume of DW transported over the Palgruža sill in these simulations amounted to 1,000–2,300 km³. Our results show a much larger variation, namely 430–4,000 km³ (Table 7). We use larger runoff modifications than Vilibić et al. (2016) and therefore obtain larger differences in DW production. It is important to note the differences between our SR runs (UERRA-SR, ERA5-SR, C_REA6-SR) in Table 7. These differ only in the atmospheric forcing, and the volume of transported DW varies from 620 to 2,000 km³ at the Palagruža sill and from 570 to 5,200 km³ at the Otranto strait. This again confirms the sensitivity of DW formation to the atmospheric products used to force the model.

Verri et al. (2018) used extremely modified runoff configurations (no runoff, realistic, 50% augmented, and doubled) to test its influence on the Adriatic-Ionian meridional overturning circulation (CMOC). Contrary to Cessi et al. (2014) they concluded that none of the river configurations can reverse its anti-estuarine character and that although the runoff affects the CMOC strength it is controlled by wind work at least as much as by the buoyancy fluxes. Similarly, our results show that the Adriatic meridional overturning circulation (AdriMOC) is influenced by river runoff. We did not explore the role of wind work, but our results show little influence of Ekman transport on the inflow through the Strait of Otranto (Figure 17) or the stream function gradient (Figure 13). On the other hand, we have found that the DW formation amplified the anti-estuarine circulation and it changed the water exchange in the Strait of Otranto from a horizontally separated regime to a more vertically separated regime. We also found out that, in addition to the river runoff, the AdriMOC exhibits sensitivity to the atmospheric products used to force the model (Figure 13). The total DW volume obtained in our experiments matches well with the values obtained by Verri et al. (2018). The latter observed that the rivers influence the stratification of the whole water column and reduce the DW production in the whole basin and that the Mediterranean inflow into the Adriatic Sea is reduced by increased river runoff. Our results confirm these findings and offer a deeper insight into the mechanisms that control these processes. We also show that these mechanisms are equally sensitive to atmospheric boundary conditions as they are to the river runoff and that the Mediterranean inflow varies by an order of magnitude depending on the choice of freshwater input and atmospheric product (Figure 16).

Many of the other models of the Adriatic Sea exhibit a primarily negative salinity bias (Benetazzo et al., 2014; Janeković et al., 2014; Mihanović et al., 2019; Oddo & Guarnieri, 2011) as does our UERRA-B baseline run. On the contrary, the NEMOMED8 (Dunić et al., 2018) exhibits significant positive salinity bias at the Palagruža sill, which was attributed to the absence of several rivers in the model. The Tiresias (Ferrarin et al., 2019) and AdriSC (Pranić et al., 2021) show positive salinity bias in the near-surface layer and negative in the rest of the water column.

4.5. The Circulation

There is a series of processes that drive the Adriatic circulation. The salinity and heat losses control the DW formation, the shelf DW (SDW) flows south and the densest DW fills the SAP, while lower density DW flows through the Strait of Otranto toward the Ionian Sea (Figure 19). The DW filling of the SAP dictates the salinity of the deep layers and produces the distinctive saw-tooth pattern of PDA as described in Querin et al. (2016). The lower density DW vein, which flows southward along the western flank of the SAP, is joined by southern Adriatic DW that forms by deep convection and is usually of larger volume but of lower density than SDW and therefore never reaches the bottom of the SAP. The DW outflow through the Strait of Otranto induces an additional inflow

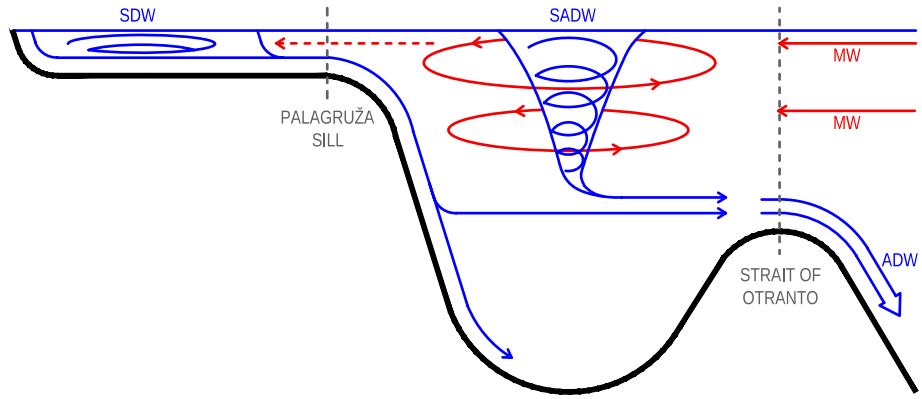

Figure 19. Schematic side-view representation of the circulation and water exchange in the Adriatic basin (not to scale). SDW - Shelf Dense Water, SADW - South Adriatic Dense Water, ADW - Adriatic Dense Water, MW - Mediterranean Water.

of salty Mediterranean water. The latter increases the salinity of the surface layers in the southern Adriatic and with occasional intrusions increases the salinity on the shelf as well, concluding a sort of a self-amplifying loop: Reduced DW production - consequence of reduced surface water salinity or/and low surface heat loss, reduces salty water inflow which further reduces the salinity of the basin. The surface layers of the basin get even fresher, while the bottom of the SAP faces salinity increase with no DW inflow and slow mixing with salty Mediterranean water. Increased DW production - consequence of high surface salinity and/or high surface heat loss, amplifies the salty water inflow through the Strait of Otranto which further increases the salinity of the surface layers. On the contrary, the SAP gets fresher due to the inflow of DW from the shelf. But if the salinity of surface layers is exaggerated to the extent that they become saltier than the inflowing Mediterranean water, the inflowing DW gets salty enough to cause an increase in the salinity of the bottom layers of the SAP.

5. Conclusions

Our modeling study provides a comprehensive overview of the processes governing the circulation of the Adriatic Sea. There is a high degree of uncertainty about the actual river discharge and also about the surface freshwater fluxes and winds in atmospheric reanalyses. On the other hand, the Adriatic circulation and salinity form a positive feedback mechanism and exhibit high sensitivity to freshwater balance and heat loss.

The model runs reveal a self-amplifying loop involving surface salinity, dense water (DW) formation and transport, inflow of Mediterranean water (MW), and its effects on surface salinity. DW formation has a strong influence on the general circulation in the Adriatic Sea. Its influence is not limited to bottom currents and water properties at the bottom of the Southern Adriatic Pit (SAP). DW production also has a strong influence on the water exchange with the Mediterranean Sea and the salinity balance in the surface layers of the basin. The models show a high sensitivity of DW formation to the overall freshwater balance (river discharge and E-P) and also to wind forcing. The amount of DW formed differs greatly between model runs. This shows that the river discharge and atmospheric forcing in Adriatic models should be chosen and calibrated with great care.

Some of the models runs that implement what appears to be the most realistic representation of river discharge and atmospheric forcing (B and ERA-SR runs) are not able to reproduce realistic DW dynamics. As the basin becomes fresher, DW production decreases and they fail to produce DW dense enough to reach the bottom of the SAP. This completely changes the dynamics of the water masses in the basin.

We also test the hypothesis proposed by Cessi et al. (2014) and implemented by Verri et al. (2018) in the Adriatic-Ionian model, which emphasizes the importance of buoyancy flux on meridional overturning circulation in semi-enclosed (or adjacent) seas. We find some indications of negative buoyancy flux amplifying anti-estuarine Adriatic meridional overturning circulation (AdriMOC) and positive buoyancy flux inducing a less anti-estuarine mode. On the other hand, there is a clear indication of DW production amplifying the anti-estuarine cells in the Southern Adriatic and the Strait of Otranto. Our results indicate that in the periods of low DW outflow,

the inflow-outflow separation in the Otranto strait is primarily horizontal while intensified DW outflow induces more vertical separation and amplifies the anti-estuarine cell.

Many of these concepts are given in the literature, whereas our study has identified and quantified the processes involved in driving the circulation of the Adriatic Sea. We have evaluated the sensitivity of each of them to freshwater input and atmospheric boundary conditions. The more than tenfold difference in some instances emphasizes the importance of reproducing realistic salinity values in Adriatic circulation models. According to our experiments, this is not an easy task, since the Adriatic salinity is a result of the interplay of several weakly constrained factors. The push toward higher spatial resolution in Adriatic modeling is undoubtedly the way forward. This is confirmed by our results as well, as they demonstrate the importance of wind resolution in DW formation and should be especially beneficial in topographically complex areas such as Kvarner bay (Figure 1). However, according to our study, the freshwater balance, which is a result of river runoff and atmospheric forcing, should be very carefully considered beforehand. Special attention should be given to the accuracy of DW production. This should ensure realistic basin dynamics.

We summarize our findings:

- The variations in surface freshwater flux caused by the choice of atmospheric forcing are of the order of magnitude of the river discharge in the Adriatic basin and have a significant impact on the freshwater balance and circulation in the model.
- The system forms a self-amplifying loop. Decreased freshwater input increases DW production, which increases salty water inflow, which in turn increases the salinity of the basin even further.
- The baseline (UERRA-B) model configuration (UERRA atmospheric forcing and fresh 100% river runoff) results in an unexpected drop in salinity and underestimated DW production. The other two atmospheric forcing options (ERA5 and COSMO_REA6) result in even less surface freshwater loss.
- The model results show that the Adriatic Sea is very sensitive to the freshwater budget. This sensitivity is not limited to surface waters but extends to the bottom of the basin.
- The freshwater balance strongly influences the water exchange through the Strait of Otranto and likely the BiOS as well (Gačić et al., 2010).
- In order to accurately reproduce the surface salinity and circulation, the Adriatic models would be advised to go beyond climatological runoff.
- The AdriMOC is strongly influenced by DW formation.

River discharge and ocean-atmosphere fluxes are notoriously difficult to assess, and both are expected to change under future climate change and anthropogenic pressures. The expected increase in droughts and floods in the coming decades could have significant impacts on DW formation and circulation of the Adriatic Sea. Our results show that a realistic freshwater balance and DW production will be difficult to obtain in Adriatic models and that the hydrography of the Adriatic Sea and its interaction with the Mediterranean Sea could change significantly in the coming decades.

Acronyms

AdriMOC	Adriatic Meridional Overturning Circulation
ADW	Adriatic Dense Water
BiOS	Adriatic-Ionian Bimodal Oscillating System
CMEMS	Copernicus Marine Service (https://marine.copernicus.eu/)
DW	Dense water
ECMWF	European Centre for Medium-Range Weather Forecasts
KV	Kvarner Bay (Croatia)
Med MFC	Mediterranean physical reanalysis—CMEMS product based on MFS
MFS	Mediterranean Forecast System
MW	Mediterranean Water
OT	Strait of Otranto
PDA	Potential Density Anomaly
SADW	South Adriatic Dense Water
SDW	Shelf Dense Water—Northern Adriatic dense water and Mid-Adriatic dense water combined
SAP	Southern Adriatic Pit

Data Availability Statement

CROCO and CROCO_TOOLS are provided by http://www.croco-ocean.org. The following data sets were used in this research:

1. MESCAN-SURFEX two-dimensional surface atmospheric analysis was obtained from ECMWF's Meteorological Archival and Retrieval System (ECMWF, 2021). This work is based on UERRA EU FP7 Collaborative Project, Grant agreement 607193.
2. ERA5 atmospheric reanalysis was retrieved from Climate Data Store (Hersbach et al., 2019).
3. COSMO_REA6 reanalysis (Source: Hans-Ertel-Center for Weather Research) was downloaded from Deutsche Wetterdienst server (HErZ, 2021).
4. Med MFC physical reanalysis (MEDSEA_MULTIYEAR_PHY_006_004) was obtained from Copernicus Marine Service (Escudier et al., 2020). This study has been conducted using E.U. Copernicus Marine Service Information; https://doi.org/10.25423/CMCC/MEDSEA_MULTIYEAR_PHY_006_004_E3R1.
5. SeaDataCloud Mediterranean climatology was downloaded from SeaDataNet web portal (Simoncelli et al., 2022). This resource was generated in framework of the SeaDataCloud project, EC H2020 grant #730960.
6. WOA2009 ocean climatology was downloaded from CROCO web portal (NODC, 2009).
7. MEDAR Mediterranean Sea climatology was downloaded from NOAA web portal (MEDAR Group, 2003).
8. Po discharge measurements were obtained from Arpae annual hydrological reports (ARPAE, 2021).
9. Isonzo (Soča) and Rižana discharge measurements were obtained from Slovenian Environment agency monthly statistics (ARSO, 2020).

Acknowledgments
M.V. would like to acknowledge the financial support from the Slovenian Research Agency (research core funding P1-0237 "Coastal research", postdoctoral project Z7-1884, and project DE-COMB J7-2599). Á. P. was partially funded by Fundação para a Ciência e a Tecnologia, I.P./MCTES through the national program (PIDDAC)–UIDB/50019/2020. The authors would like to thank fellow researchers who offered insight, advice, and help in many useful discussions: Stefano Querin (OGS), Matjaž Ličer (ARSO, NIB), Vlado Malačič (NIB), Jurij Jerman (ARSO), Sašo Petan (ARSO), Gregor Kosec (IJS), Ana Machado (IDL, IPMA), and Sandra Plecha (IDL).

References

ARPAE. (2021). Arpae Emilia Romagna: Hydrological reports. [Dataset]. Retrieved from https://www.arpae.it/it/temi-ambientali/meteo/report-meteo/annali-idrologici

ARSO. (2020). Slovenian Environment Agency: Hydrological Archive [Dataset]. Retrieved from https://www.arso.gov.si/vode/podatki/arhiv/hidroloski_arhiv.html

Bazile, E., Abida, R., Verelle, A., Le Moigne, P., & Szczypta, C. (2017). MESCAN-SURFEX surface analysis. Deliverable D2.8 of the UERRA project. Project 607193 UERRA. Retrieved from http://www.uerra.eu/publications/deliverable-reports.html

Benetazzo, A., Bergamasco, A., Bonaldo, D., Falcieri, F., Sclavo, M., Langone, L., & Carniel, S. (2014). Response of the Adriatic Sea to an intense cold air outbreak: Dense water dynamics and wave-induced transport. *Progress in Oceanography*, *128*, 115–138. https://doi.org/10.1016/j.pocean.2014.08.015

Bergamasco, A., Oguz, T., & Malanotte-Rizzoli, P. (1999). Modeling dense water mass formation and winter circulation in the northern and central Adriatic Sea. *Journal of Marine Systems*, *20*(1–4), 279–300. https://doi.org/10.1016/s0924-7963(98)00087-6

Berntsen, J., & Oey, L.-Y. (2010). Estimation of the internal pressure gradient in σ-coordinate ocean models: Comparison of second-, fourth-, and sixth-order schemes. *Ocean Dynamics*, *60*(2), 317–330. https://doi.org/10.1007/s10236-009-0245-y

Bertotti, L., & Cavaleri, L. (2009). Wind and wave predictions in the Adriatic Sea. *Journal of Marine Systems*, *78*, S227–S234. https://doi.org/10.1016/j.jmarsys.2009.01.018

Bollmeyer, C. (2015). *A high-resolution regional reanalysis for Europe and Germany (Unpublished doctoral dissertation)*. Universitäts-und Landesbibliothek.

Bollmeyer, C., Keller, J., Ohlwein, C., Wahl, S., Crewell, S., Friederichs, P., et al. (2015). Towards a high-resolution regional reanalysis for the European CORDEX domain. *Quarterly Journal of the Royal Meteorological Society*, *141*(686), 1–15. https://doi.org/10.1002/qj.2486

Bressan, L., Valentini, A., Paccagnella, T., Montani, A., Marsigli, C., & Tesini, M. S. (2017). Sensitivity of sea-level forecasting to the horizontal resolution and sea surface forcing for different configurations of an oceanographic model of the Adriatic Sea. *Advances in Science and Research*, *14*, 77–84. https://doi.org/10.5194/asr-14-77-2017

Carniel, S., Benetazzo, A., Bonaldo, D., Falcieri, F. M., Miglietta, M. M., Ricchi, A., & Sclavo, M. (2016). Scratching beneath the surface while coupling atmosphere, ocean and waves: Analysis of a dense water formation event. *Ocean Modelling*, *101*, 101–112. https://doi.org/10.1016/j.ocemod.2016.03.007

Carniel, S., Bonaldo, D., Benetazzo, A., Bergamasco, A., Boldrin, A., Falcieri, F. M., et al. (2016). Off-shelf fluxes across the southern Adriatic margin: Factors controlling dense-water-driven transport phenomena. *Marine Geology*, *375*, 44–63. https://doi.org/10.1016/j.margeo.2015.08.016

Cavaleri, L., & Bertotti, L. (1997). In search of the correct wind and wave fields in a minor basin. *Monthly Weather Review*, *125*(8), 1964–1975. https://doi.org/10.1175/1520-0493(1997)125<1964:isotcw>2.0.co;2

Cessi, P., Pinardi, N., & Lyubartsev, V. (2014). Energetics of semienclosed basins with two-layer flows at the strait. *Journal of Physical Oceanography*, *44*(3), 967–979. https://doi.org/10.1175/jpo-d-13-0129.1

Cozzi, S., & Giani, M. (2011). River water and nutrient discharges in the northern Adriatic Sea: Current importance and long term changes. *Continental Shelf Research*, *31*(18), 1881–1893. https://doi.org/10.1016/j.csr.2011.08.010

Cushman-Roisin, B., Gacic, M., Poulain, P.-M., & Artegiani, A. (2001). *Physical oceanography of the Adriatic Sea: Past, present and future*. Springer Science & Business Media.

Cushman-Roisin, B., & Naimie, C. E. (2002). A 3D finite-element model of the Adriatic tides. *Journal of Marine Systems*, *37*(4), 279–297. https://doi.org/10.1016/s0924-7963(02)00204-x

Dee, D. P., Uppala, S. M., Simmons, A. J., Berrisford, P., Poli, P., Kobayashi, S., et al. (2011). The ERA-Interim reanalysis: Configuration and performance of the data assimilation system. *Quarterly Journal of the Royal Meteorological Society*, *137*(656), 553–597. https://doi.org/10.1002/qj.828

Denamiel, C., Tojčić, I., Pranić, P., & Vilibić, I. (2022). Modes of the BiOS-driven Adriatic Sea thermohaline variability. *Climate Dynamics*, 1–17. https://doi.org/10.1007/s00382-022-06178-4

Denamiel, C., Tojčić, I., & Vilibić, I. (2020). Far future climate (2060–2100) of the northern Adriatic air–sea heat transfers associated with extreme bora events. *Climate Dynamics*, *55*(11), 3043–3066. https://doi.org/10.1007/s00382-020-05435-8

Denamiel, C., Tojčić, I., & Vilibić, I. (2022). Meteotsunamis in orography-free, flat bathymetry and warming climate conditions. *Journal of Geophysical Research: Oceans*, *127*(1), e2021JC017386. https://doi.org/10.1029/2021jc017386

Doms, G., & Schättler, U. (2002). A description of the nonhydrostatic regional model LM. Part I: Dynamics and numerics. *COSMO Newsletter*, *2*, 225–235.

Dottori, F., Martina, M., & Todini, E. (2009). A dynamic rating curve approach to indirect discharge measurement. *Hydrology and Earth System Sciences*, *13*(6), 847–863. https://doi.org/10.5194/hess-13-847-2009

Dunić, N., Vilibić, I., Šepić, J., Mihanović, H., Sevault, F., Somot, S., et al. (2019). Performance of multi-decadal ocean simulations in the Adriatic Sea. *Ocean Modelling*, *134*, 84–109. https://doi.org/10.1016/j.ocemod.2019.01.006

Dunić, N., Vilibić, I., Šepić, J., Somot, S., & Sevault, F. (2018). Dense water formation and BiOS-induced variability in the Adriatic Sea simulated using an ocean regional circulation model. *Climate Dynamics*, *51*(3), 1211–1236. https://doi.org/10.1007/s00382-016-3310-5

ECMWF. (2021). MESCAN-SURFEX [Dataset]. MediumRange. Retrieved from https://apps.ecmwf.int/datasets/data/uerra-mescan-surfex/levtype=sfc/stream=oper/type=an/

Escudier, R., Clementi, E., Omar, M., Cipollone, A., Pistoia, J., Aydogdu, A., et al. (2020). Mediterranean Sea physical reanalysis (CMEMS MED-Currents)(version 1) [Dataset]. Copernicus Monitoring Environment Marine Service (CMEMS). Retrieved from https://resources.marine.copernicus.eu/products

Fairall, C. W., Bradley, E. F., Hare, J., Grachev, A. A., & Edson, J. B. (2003). Bulk parameterization of air–sea fluxes: Updates and verification for the COARE algorithm. *Journal of Climate*, *16*(4), 571–591. https://doi.org/10.1175/1520-0442(2003)016<0571:bpoasf>2.0.co;2

Fairall, C. W., Bradley, E. F., Rogers, D. P., Edson, J. B., & Young, G. S. (1996). Bulk parameterization of air-sea fluxes for tropical ocean-global atmosphere coupled-ocean atmosphere response experiment. *Journal of Geophysical Research*, *101*(C2), 3747–3764. https://doi.org/10.1029/95jc03205

Ferrarin, C., Davolio, S., Bellafiore, D., Ghezzo, M., Maicu, F., Mc Kiver, W., et al. (2019). Cross-scale operational oceanography in the Adriatic Sea. *Journal of Operational Oceanography*, *12*(2), 86–103. https://doi.org/10.1080/1755876x.2019.1576275

Ferrarin, C., Valentini, A., Vodopivec, M., Klaric, D., Massaro, G., Bajo, M., et al. (2020). Integrated sea storm management strategy: The 29 October 2018 event in the Adriatic Sea. *Natural Hazards and Earth System Sciences*, *20*(1), 73–93. https://doi.org/10.5194/nhess-20-73-2020

Gačić, M., Borzelli, G. E., Civitarese, G., Cardin, V., & Yari, S. (2010). Can internal processes sustain reversals of the ocean upper circulation? The Ionian Sea example. *Geophysical Research Letters*, *37*(9). https://doi.org/10.1029/2010GL043216

Gačić, M., Ursella, L., Kovačević, V., Menna, M., Malačič, V., Bensi, M., et al. (2021). Impact of dense-water flow over a sloping bottom on open-sea circulation: Laboratory experiments and an Ionian sea (mediterranean) example. *Ocean Science*, *17*(4), 975–996. https://doi.org/10.5194/os-17-975-202

Giorgi, F., Jones, C., & Asrar, G. R. (2009). Addressing climate information needs at the regional level: The CORDEX framework. *World Meteorological Organization Bulletin*, *58*(3), 175.

Hersbach, H., Bell, B., Berrisford, P., Biavati, G., Horányi, A., Muñoz Sabater, J., & Thépaut, J.-N. (2019). ERA5 monthly averaged data on single levels from 1979 to present. Copernicus Climate Change Service (C3S) [Dataset]. Climate Data Store (CDS). Retrieved from https://doi.org/10.24381/cds.f17050d7

Hersbach, H., Bell, B., Berrisford, P., Hirahara, S., Horányi, A., Muñoz-Sabater, J., et al. (2020). The ERA5 global reanalysis. *Quarterly Journal of the Royal Meteorological Society*, *146*(730), 1999–2049. https://doi.org/10.1002/qj.3803

HErZ. (2021). COSMO_REA6 [Dataset]. HansErtel-Centre. Retrieved from https://opendata.dwd.de/climate_environment/REA/COSMO_REA6/

Janeković, I., Mihanović, H., Vilibić, I., & Tudor, M. (2014). Extreme cooling and dense water formation estimates in open and coastal regions of the Adriatic Sea during the winter of 2012. *Journal of Geophysical Research: Oceans*, *119*(5), 3200–3218. https://doi.org/10.1002/2014JC009865

Ličer, M., Estival, S., Reyes-Suarez, C., Deponte, D., & Fettich, A. (2020). Lagrangian modelling of a person lost at sea during the Adriatic scirocco storm of 29 October 2018. *Natural Hazards and Earth System Sciences*, *20*(8), 2335–2349. https://doi.org/10.5194/nhess-20-2335-2020

Ličer, M., Smerkol, P., Fettich, A., Ravdas, M., Papapostolou, A., Mantziafou, A., et al. (2016). Modeling the ocean and atmosphere during an extreme bora event in northern Adriatic using one-way and two-way atmosphere–ocean coupling. *Ocean Science*, *12*(1), 71–86. https://doi.org/10.5194/os-12-71-2016

Madec, G., & Team, N. S. (2022). Nemo ocean engine (Computer software manual No. 27). *Zenodo*. https://doi.org/10.5281/zenodo.1464816

Malačič, V. (2019). Wind direction measurements on Moored coastal buoys. *Journal of Atmospheric and Oceanic Technology*, *36*(7), 1401–1418. https://doi.org/10.1175/JTECH-D-18-0171.1

Malačič, V., Petelin, B., & Vodopivec, M. (2012). Topographic control of wind-driven circulation in the northern Adriatic. *Journal of Geophysical Research*, *117*(C6). https://doi.org/10.1029/2012JC008063

Malačič, V., Viezzoli, D., & Cushman-Roisin, B. (2000). Tidal dynamics in the northern Adriatic Sea. *Journal of Geophysical Research*, *105*(C11), 26265–26280. https://doi.org/10.1029/2000JC900123

Mantziafou, A., & Lascaratos, A. (2008). Deep-water formation in the Adriatic Sea: Interannual simulations for the years 1979–1999. *Deep Sea Research Part I: Oceanographic Research Papers*, *55*(11), 1403–1427. https://doi.org/10.1016/j.dsr.2008.06.005

MEDAR Group. (2003). MEDAR MEDATLAS DATABASE: Temperature, salinity, and nutrient observations collected in the Mediterranean and Black Seas as part of the MEDAR/MEDATLAS project, 1889-2000 (NCEI Accession 0000996) [Dataset]. NOAA National Centers for Environmental Information. Retrieved from https://www.ncei.noaa.gov/archive/accession/0000996

Mihanović, H., Janeković, I., Vilibić, I., Kovačević, V., & Bensi, M. (2019). Modelling interannual changes in dense water formation on the northern Adriatic shelf. In *Meteorology and climatology of the mediterranean and black seas* (pp. 345–361). Springer. https://doi.org/10.1007/978-3-030-11958-4_21

Mihanović, H., Vilibić, I., Carniel, S., Tudor, M., Russo, A., Bergamasco, A., et al. (2013). Exceptional dense water formation on the Adriatic shelf in the winter of 2012. *Ocean Science*, *9*(3), 561–572. https://doi.org/10.5194/os-9-561-2013

Mihanović, H., Vilibić, I., Šepić, J., Matić, F., Ljubešić, Z., Mauri, E., et al. (2021). Observation, preconditioning and recurrence of exceptionally high salinities in the Adriatic Sea. *Frontiers in Marine Science*, *8*, 834. https://doi.org/10.3389/fmars.2021.672210

Niermann, D., Borsche, M., Kaiser-Weiss, A., Lussana, C., Tveito, O. E., Francesco, I., & Verver, G. (2018). Report for Deliverable 3.8 (D3.8): User friendly synthesis report on evaluation and uncertainty of regional reanalyses. *Project 607193 UERRA*. Retrieved from http://www.uerra.eu/publications/deliverable-reports.html

NODC. (2009). World Ocean Atlas 2009 (WOA09) [Dataset]. Ocean Climate Laboratory of the National Oceanographic Data Center (U.S.). Retrieved from https://www.croco-ocean.org/download/datasets/

Oddo, P., & Guarnieri, A. (2011). A study of the hydrographic conditions in the Adriatic Sea from numerical modelling and direct observations (2000–2008). *Ocean Science*, *7*(5), 549–567. https://doi.org/10.5194/os-7-549-2011

Oddo, P., Pinardi, N., & Zavatarelli, M. (2005). A numerical study of the interannual variability of the Adriatic Sea (2000–2002). *Science of the Total Environment*, *353*(1–3), 39–56. https://doi.org/10.1016/j.scitotenv.2005.09.061

Pedlosky, J. (1987). *Geophysical fluid dynamics* (Vol. 710). Springer.

Penven, P., Marchesiello, P., Debreu, L., & Lefèvre, J. (2008). Software tools for pre-and post-processing of oceanic regional simulations. *Environmental Modelling & Software*, *23*(5), 660–662. https://doi.org/10.1016/j.envsoft.2007.07.004

Pinardi, N., Allen, I., Demirov, E., De Mey, P., Korres, G., Lascaratos, A., et al. (2003). The Mediterranean ocean forecasting system: First phase of implementation (1998–2001). *Annales Geophysicae*, *21*, 3–20. https://doi.org/10.5194/angeo-21-3-2003

Pinardi, N., Arneri, E., Crise, A., Ravaioli, M., & Zavatarelli, M. (2006). The physical, sedimentary and ecological structure and variability of shelf areas in the mediterranean sea (27). *The Sea*, *14*, 1243–1330.

Poulain, P.-M., Mauri, E., & Ursella, L. (2004). Unusual upwelling event and current reversal off the Italian adriatic coast in summer 2003. *Geophysical Research Letters*, *31*(5). https://doi.org/10.1029/2003gl019121

Pranić, P., Denamiel, C., & Vilibić, I. (2021). Performance of the Adriatic Sea and coast (AdriSC) climate component–a COAWST V3. 3-based one-way coupled atmosphere–ocean modelling suite: Ocean results. *Geoscientific Model Development*, *14*(10), 5927–5955. https://doi.org/10.5194/gmd-14-5927-2021

Querin, S., Bensi, M., Cardin, V., Solidoro, C., Bacer, S., Mariotti, L., et al. (2016). Saw-tooth modulation of the deep-water thermohaline properties in the southern Adriatic Sea. *Journal of Geophysical Research: Oceans*, *121*(7), 4585–4600. https://doi.org/10.1002/2015jc011522

Querin, S., Cossarini, G., & Solidoro, C. (2013). Simulating the formation and fate of dense water in a midlatitude marginal sea during normal and warm winter conditions. *Journal of Geophysical Research: Oceans*, *118*(2), 885–900. https://doi.org/10.1002/jgrc.20092

Raicich, F. (1994). *Note on the flow rates of the Adriatic rivers (Tech. Rep. No. RF 02/94)*. CNR. Istituto sperimentale talassografico.

Rew, R., & Davis, G. (1990). NetCDF: An interface for scientific data access. *IEEE Computer Graphics and Applications*, *10*(4), 76–82. https://doi.org/10.1109/38.56302

Ricchi, A., Miglietta, M. M., Falco, P. P., Benetazzo, A., Bonaldo, D., Bergamasco, A., et al. (2016). On the use of a coupled ocean–atmosphere–wave model during an extreme cold air outbreak over the Adriatic Sea. *Atmospheric Research*, *172*, 48–65. https://doi.org/10.1016/j.atmosres.2015.12.023

Russo, A., Coluccelli, A., Carniel, S., Benetazzo, A., Valentini, A., Paccagnella, T., et al. (2013). Operational models hierarchy for short term marine predictions: The Adriatic Sea example. In 2013 mts/ieee oceans-bergen (pp. 1–6). https://doi.org/10.1109/oceans-bergen.2013.6608139

Signell, R. P., Carniel, S., Cavaleri, L., Chiggiato, J., Doyle, J. D., Pullen, J., & Sclavo, M. (2005). Assessment of wind quality for oceanographic modelling in semi-enclosed basins. *Journal of Marine Systems*, *53*(1–4), 217–233. https://doi.org/10.1016/j.jmarsys.2004.03.006

Sikirić, M. D., Janeković, I., & Kuzmić, M. (2009). A new approach to bathymetry smoothing in sigma-coordinate ocean models. *Ocean Modelling*, *29*(2), 128–136. https://doi.org/10.1016/j.ocemod.2009.03.009

Simoncelli, S., Oliveri, P., & Mattia, G. (2022). SeaDataCloud Mediterranean Sea - V2, Temperature and Salinity Climatology. [Dataset]. Retrieved from https://www.seadatanet.org/Products%23/metadata/3f8eaace%2D9f9b%2D4b1b%2Da7a4-9c55270e205a

Simoncelli, S., Pinardi, N., Oddo, P., Mariano, A. J., Montanari, G., Rinaldi, A., & Deserti, M. (2011). Coastal rapid environmental assessment in the northern Adriatic Sea. *Dynamics of Atmospheres and Oceans*, *52*(1–2), 250–283. https://doi.org/10.1016/j.dynatmoce.2011.04.004

Soci, C., Bazile, E., Besson, F., & Landelius, T. (2016). High-resolution precipitation re-analysis system for climatological purposes. *Tellus A: Dynamic Meteorology and Oceanography*, *68*(1), 29879. https://doi.org/10.3402/tellusa.v68.29879

Soufflet, Y., Marchesiello, P., Lemarié, F., Jouanno, J., Capet, X., Debreu, L., & Benshila, R. (2016). On effective resolution in ocean models. *Ocean Modelling*, *98*, 36–50. https://doi.org/10.1016/j.ocemod.2015.12.004

Verri, G., Pinardi, N., Oddo, P., Ciliberti, S. A., & Coppini, G. (2018). River runoff influences on the Central Mediterranean overturning circulation. *Climate Dynamics*, *50*(5), 1675–1703. https://doi.org/10.1007/s00382-017-3715-9

Vested, H. J., Berg, P., & Uhrenholdt, T. (1998). Dense water Formation in the northern adriatic. *Journal of Marine Systems*, *18*(1–3), 135–160. https://doi.org/10.1016/s0924-7963(98)00009-8

Vilibić, I., Mihanović, H., Janeković, I., & Šepić, J. (2016). Modelling the formation of dense water in the northern Adriatic: Sensitivity studies. *Ocean Modelling*, *101*, 17–29. https://doi.org/10.1016/j.ocemod.2016.03.001

Vilibić, I., Zemunik, P., Šepić, J., Dunić, N., Marzouk, O., Mihanović, H., et al. (2019). Present climate trends and variability in thermohaline properties of the northern adriatic shelf. *Ocean Science*, *15*(5), 1351–1362. https://doi.org/10.5194/os-15-1351-2019